ChemComm

Chemical Communications

rsc.li/chemcomm

ROYAL SOCIETY
OF CHEMISTRY
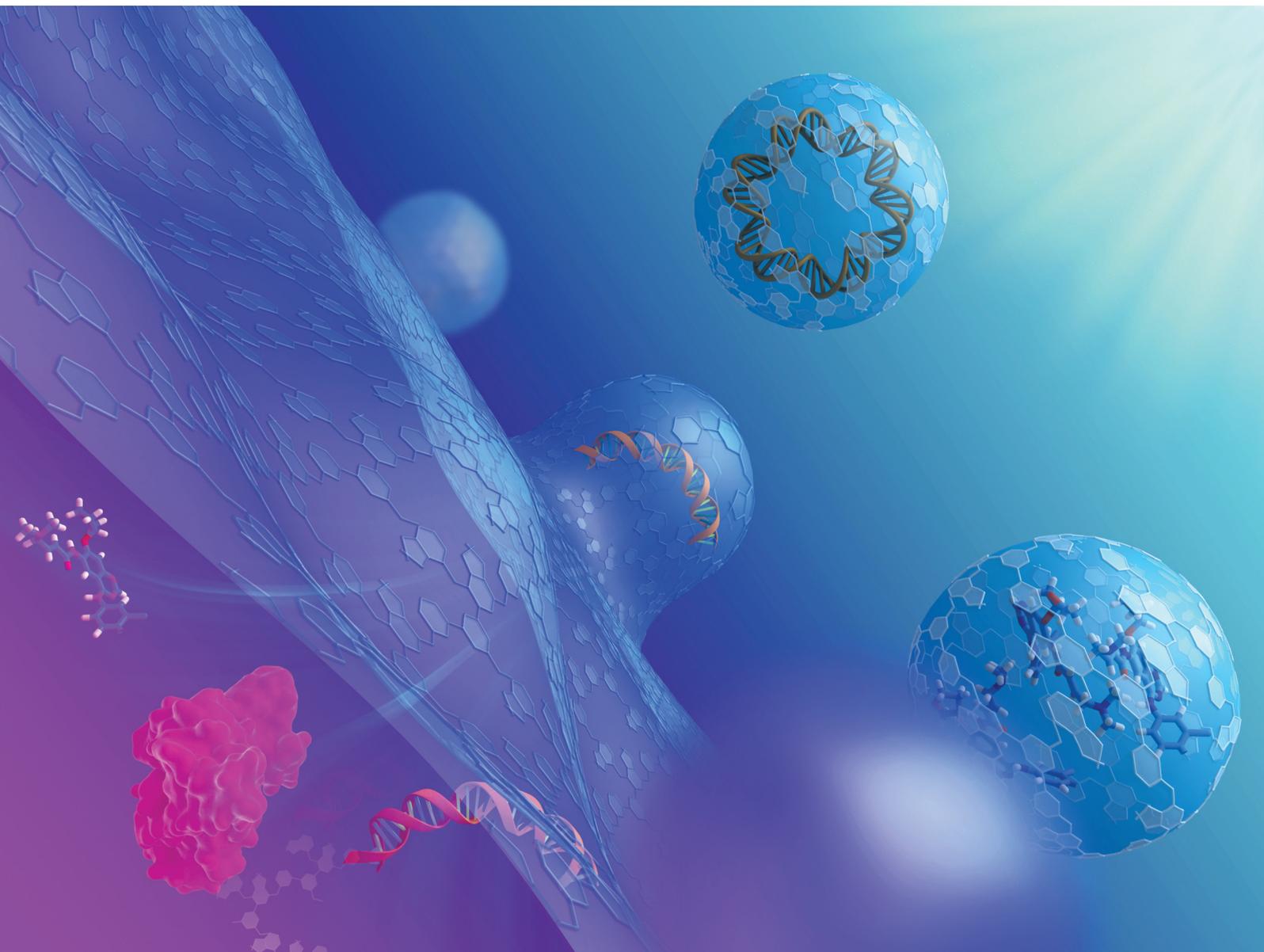
FEATURE ARTICLE
Hélder A. Santos *et al.*
Acetalated dextran based nano- and microparticles:
synthesis, fabrication, and therapeutic applications

FEATURE ARTICLE

Check for updates

Acetalated dextran based nano- and microparticles: synthesis, fabrication, and therapeutic applications

Shiqi Wang, [ID] [a] Flavia Fontana,[a] Mohammad-Ali Shahbazi [ID] [abc] and Hélder A. Santos [ID] *[ad]

Acetalated dextran (Ac-DEX) is a pH-responsive dextran derivative polymer. Prepared by a simple acetalation reaction, Ac-DEX has tunable acid-triggered release profile. Despite its relatively short research history, Ac-DEX has shown great potential in various therapeutic applications. Furthermore, the recent functionalization of Ac-DEX makes versatile derivatives with additional properties. Herein, we summarize the cutting-edge development of Ac-DEX and related polymers. Specifically, we focus on the chemical synthesis, nano- and micro-particle fabrication techniques, the controlled-release mechanisms, and the rational design Ac-DEX-based of drug delivery systems in various biomedical applications. Finally, we briefly discuss the challenges and future perspectives in the field.

Introduction

Dextran is a family of natural polysaccharides produced from microbial origins.[1] Depending on its origin, dextran has main chains consisting of α-1,6-glucosidic linkages with different lengths and different ratios of branches *via* 1,3 linkages.[2]

[a] *Drug Research Program, Division of Pharmaceutical Chemistry and Technology, Faculty of Pharmacy, University of Helsinki, FI-00014 Helsinki, Finland. E-mail: helder.santos@helsinki.fi*

[b] *Zanjan Pharmaceutical Nanotechnology Research Center (ZPNRC), Zanjan University of Medical Sciences, 45139-56184 Zanjan, Iran*

[c] *Department of Pharmaceutical Nanotechnology, School of Pharmacy, Zanjan University of Medical Sciences, 45139-56184 Zanjan, Iran*

[d] *Helsinki Institute of Life Science (HiLIFE), University of Helsinki, FI-00014 Helsinki, Finland*

Dextran is well-known for its biocompatibility and biodegradability, and has been used since the 1940s as a blood volume expander administrated intravenously.[3] Recent studies have further explored its potential for drug delivery applications by chemical conjugation and functionalization, which enable dextran to have desirable physicochemical properties and stimuli-responsiveness for controlled drug release behaviour.[4–7]
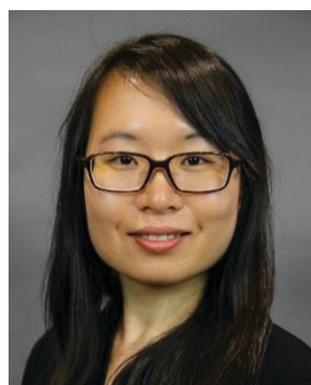
Acetalated dextran (Ac-DEX) is one of the most investigated dextran derivatives. It was first reported by Bachelder *et al.* in 2008,[8] synthesized by a simple one-step reaction, between dextran and 2-methoxypropene, catalysed by pyridinium *p*-toluenesulfonate (PPTS). After acetalation of pendant hydroxyl groups on dextran, the resulted polymer (Ac-DEX) becomes insoluble in water, but soluble in organic solvents such as ethanol, ethyl acetate, and dichloromethane.[8] Furthermore, these acetal groups are prone

Shiqi Wang received her Bachelor and Master degrees from Tsinghua University China in 2012 and 2014 respectively. Then she moved to Imperial College London as a Marie Curie Early Stage Researcher in the department of chemical engineering, where she got her PhD degree in 2018. Afterwards, she joined University of Helsinki as a postdoctoral researcher in Prof. Santos' group. Her research interests include developing stimuli-responsive polymeric materials for drug delivery applications.

Shiqi Wang

Flavia Fontana earned her PhD cum laude in pharmacy at the University of Helsinki. Currently, she is a postdoctoral researcher under the supervision of Prof. Santos. She works at the interface between materials science and immunology, focusing on cancer immunotherapy and chronic inflammation.

Flavia Fontana

to acidic hydrolysis, which recovers dextran with methanol and acetone as degradation products.[8] The hydrophobicity and solubility in organic solvents makes Ac-DEX favourable for drug encapsulation by both precipitation and emulsion techniques, and the acid-triggered degradation makes it possible to release the drug in specific acidified conditions, such as endosomal compartments, tumour microenvironment and inflamed area.[9]

As a result of its relatively simple preparation, fabrication and controllable degradation, the past decade has witnessed a growing interest in Ac-DEX-based drug delivery systems with a considerable amount of literature published every year. For example, there is a review about Ac-DEX by Bachelder *et al.* in 2016,[10] focusing on the original development of this polymer and its applications especially in vaccine delivery.

In this feature article, we summarize the state-of-the-art progress in this field, and provide a systematic and comprehensive analysis of Ac-DEX, including polymer synthesis, nano- and micro-particles fabrication, controlled release behaviour and therapeutic applications. Especially, we highlight the development of new Ac-DEX derivatives, the fabrication of complex Ac-DEX composite particles using microfluidic techniques, and the emerging therapeutic applications by Ac-DEX based nano- and micro-particles. In the end, we briefly summarize the current challenges in the field, and provide critical insights into the future developments.

Acetalated dextran: synthesis and functional derivatives

As briefly introduced in the previous section, the original synthetic scheme of Ac-DEX is shown in Fig. 1a. There are both cyclic and acyclic acetal groups on Ac-DEX. The formation of acyclic acetals was fast and kinetically favoured.[11] According to the detailed kinetic study, more than 80% of hydroxyl groups have been substituted by acyclic acetals within 5 min.[11] In contrast, the formation of cyclic acetals was thermodynamically

favourable.[11] When prolonging the reaction time, cyclic acetals gradually replaced acyclic ones.[11] Therefore, by tuning reaction time, Ac-DEX with different ratios of cyclic and acyclic acetals can be obtained. The ratio of cyclic and acyclic acetals is an important structural character of Ac-DEX, because it has a direct impact on the polymer degradation rate. Acyclic acetals hydrolyse rapidly into methanol and acetone, while cyclic acetals hydrolyse into acetone slowly.[11] By adjusting the ratio of cyclic and acyclic acetals, it is possible to control the polymer degradation half-life.

Apart from 2-methoxypropene, other enol ethers have been used for dextran acetalation (Fig. 1b). For example, Ace-DEX, synthesized from 2-ethoxypropene, have been thoroughly investigated.[12–17] Compared with Ac-DEX, Ace-DEX has similar physiochemical properties and pH-dependent degradation by hydrolysis.[12] The most significant difference is the degradation products (acetone and ethanol), instead of acetone and methanol as in the case of Ac-DEX.[12] Ethanol is less toxic than methanol, making Ace-DEX possible for high dosing *in vivo* applications.[12]

A recent publication expanded the Ac-DEX family by incorporating 5-, 6-, and 7-membered ring cyclic enol ethers in the synthesis[18] (Fig. 1b). The reaction kinetics of 5- and 7-membered ring cyclic enol ethers were similar to Ac-DEX, featuring fast acyclic acetal formation, followed by a gradual conversion to cyclic acetals.[18] However, the reaction with methoxycyclohexene was relatively slow.[18] A high acyclic acetal coverage was maintained over the reaction, with slowly increasing cyclic acetal substitution.[18] As a result of the hydrophobicity of cyclic acetals, spirocyclic Ac-DEX become water-insoluble and organic-soluble at 20–40% hydroxyl substitution, while for Ac-DEX, only >70% substitution enables organic solubility.[18] The lower acetal coverage means there are more free hydroxyls for further functionalization, and less hydrolysis byproducts generated during degradation.[18]

In addition to the investigation on the acetals groups, Ac-DEX functionalization on hydroxyl groups have been developed to maximize its potential for drug delivery. A noticeable example is

Mohammad-Ali Shahbazi received his PhD in 2015 from University of Helsinki, Finland, where he worked on porous materials for drug delivery to cancer tissues. He is currently a postdoc scientist in the Faculty of Pharmacy, University of Helsinki, working on therapeutic microdevices for autoimmune diseases. He is an expert in oral peptide delivery, fabrication of cell-mimicking carriers, and bio-materials for tissue engineering. His current research interest lies in nano-based regenerative hydrogels for wound healing, bone repair, and long-term drug delivery.

Mohammad-Ali Shahbazi

Hélder A. Santos obtained his Doctor of Science in Technology (Chemical Engineering) in 2007 from the Helsinki University of Technology. Currently, he is a Full Professor in Pharmaceutical Nanotechnology at the Faculty of Pharmacy, University of Helsinki, and Head of the Nanomedicines and Biomedical Engineering Lab. His scientific expertise lies in the development of nanoparticles/ nanomedicines for biomedical applications, particularly porous silicon and polymeric-based nanomaterials for simultaneous controlled drug delivery, diagnostic, and therapy for cancer, diabetes, and cardiovascular diseases.
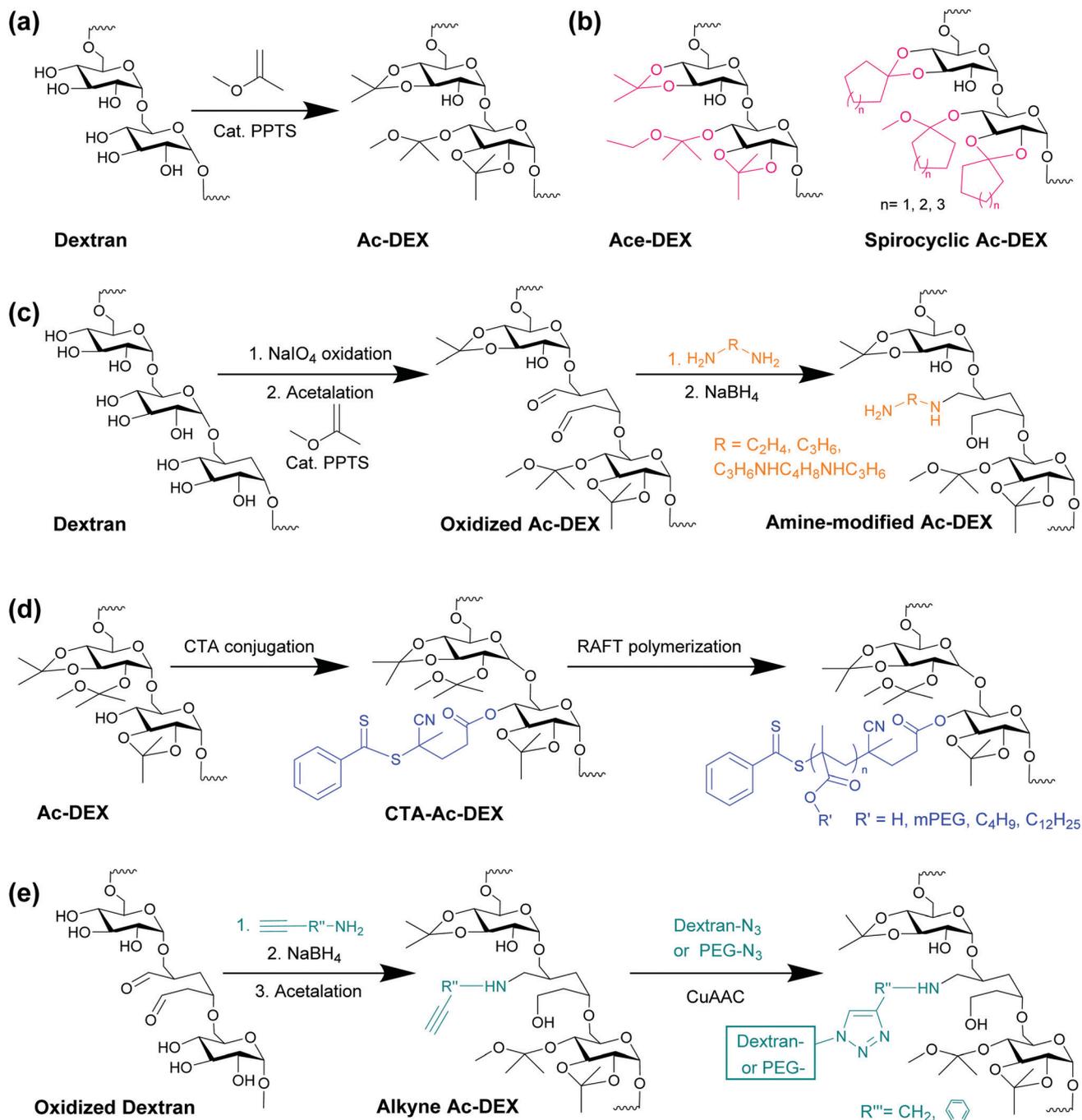
Hélder A. Santos

Fig. 1 Schematic synthesis reactions of Ac-DEX and its representative derivatives. (a) Ac-DEX, synthesized from dextran and 2-methoxypropene, catalysed by PPTS.[8] (b) Other acetal modified dextran. Ace-DEX, synthesized from dextran and 2-ethoxypropene.[12] Spiralcyclic Ac-DEX, synthesized from dextran and cyclic enol ethers (1-methoxycyclopentene, 1-methoxycyclohexene, or 1-methoxycycloheptene).[18] (c) Amine-modified dextran synthesis, by partially oxidation of dextran, acetalation, imine bond formation and reduction.[19,20,23] (d) Grafted Ac-DEX polymers by conjugation of a chain transfer agent (CTA), followed by reversible addition–fragmentation chain-transfer (RAFT) polymerization.[26,28,29] (e) Amphiphilic Ac-DEX block copolymers, synthesized by Cu(I)-catalyzed azide–alkyne cycloaddition (CuAAC) click reaction.[31,32]

cationic Ac-DEX (Fig. 1c). By partial oxidation, a small portion of hydroxyl groups on dextran are converted to aldehyde, followed by acetalation. Finally, the oxidized Ac-DEX is modified by different primary diamines, with the imine bond reduced by sodium borohydride. The first report of cationic Ac-DEX was by Cohen *et al.*, using spermine.[19] By elemental analysis, there were on average 6.6 spermine per 100 anhydroglucose units.[19] Another study used ethylenediamine for modification, yielding a series of polymers with 7.4–10.1 primary amines per 100 anhydroglucose units.[20] The positively charged Ac-DEX overcomes the difficulty in encapsulating anionic macromolecule, such as siRNA, and provides functional amine groups after particle formation for

further conjugation of targeting moieties or polyethylene glycol (PEG) to enhance the stability.[21–24]

Ac-DEX-based copolymers represent another category of functionalized Ac-DEX family. According to the synthetic strategy, copolymers are synthesized by either "grafting from" or "grafting to" approaches. On one hand, "grafting from" refers to covalently conjugation of a polymerization initiator on Ac-DEX, which allows the polymer chains to grow *in situ* (Fig. 1d). "Grafting to", on the other hand, refers to coupling the Ac-DEX with another end-functionalized polymer, *via* a highly efficient reaction, such as Cu(ı)-catalyzed azide–alkyne cycloaddition (CuAAC) (Fig. 1e). Generally speaking, "grafting to" strategy has lower grafting density than "grafting from", due to steric hindrance from both polymers.[25]

The first Ac-DEX-grafted copolymers synthesized by "grafting from" approach was reported by Duong *et al. via* living radial polymerization.[26] Specifically, they conjugated a chain transfer agent (CTA) on the hydroxyl residuals of Ac-DEX, followed by reversible addition–fragmentation chain-transfer (RAFT) polymerization of oligo(ethylene glycol)methyl ether methacrylate (OEGMA).[26] As a result of the well-controlled nature of RAFT polymerization, the chain length of the grafted polymer can be tuned by reaction time.[27] The amphiphilic comb-like copolymer self-assembled in water and formed different morphologies, including vesicles, worm-like nanorods and spherical nanoparticles (NPs).[26] The increase in the hydrophilic chain length led to a decrease in the hydrodynamic diameter, and favored the formation of the particles.[26] Santos' lab has recently expanded the Ac-DEX-based copolymers using RAFT polymerization. We grafted different endosomolytic polymers, *i.e.*, poly(lauryl methacrylate-*co*-methacrylic acid) or poly(butyl methacrylate-*co*-methacrylic acid).[28,29] The copolymers maintained the endosomal escape activities by destabilizing endosomal membranes, and released the payloads following the hydrolysis of Ac-DEX.[28,29]

The "grafting to" approach has also been investigated for Ac-DEX functionalization. Several reports used CuAAC click reaction, which is regarded to be highly efficient and simple.[30] Specifically, dextran was first partially oxidized and modified with alkyne containing primary amines (Fig. 1e).[31,32] Then the alkyne dextran was acetalated to generate alkyne Ac-DEX, which reacted with azide-terminated polymers, such as PEG or dextran, by CuAAC.[31,33] Despite the high efficiency of CuAAC, all reports have used elevated temperature (50 or 60 °C) and 72 h reaction time.[31–33] Further removal of copper(ı) catalyst by dialysis took another 3–4 days,[31–33] which is very time-consuming. There were also side products formation, which undermined the reaction efficiency.[31] To avoid copper catalysts and simplified the reaction procedure, Breitenbach *et al.* used a thiol-exchange ligation to conjugate dextran to Ac-DEX.[34] Thiol-terminated dextran and pyridyl disulfide modified Ac-DEX were prepared separately, and the ligation was performed at room temperature for 24 h.[34] It was found that the metal-free ligation could achieve complete thiol-exchange without side reactions.[34] The resulted polymer had double-stimulus-responsiveness due to the acetals groups from Ac-DEX and the disulfide linkages formed in the thiol-exchange reaction.[34]

Nano- and micro-particles fabrication

The applications of dextran and its chemical derivatives in the therapeutic field benefit from the formulation into micro/nano-particles, scaffolds, confetti, and fibres. This review will focus on micro/nano-particles. The main fabrication methods are nanoprecipitation, single emulsion, double emulsion, electrospray, and spray drying. We provide a brief introduction of the theoretical basis of each of the techniques, and elicit how they were used to prepare Ac-DEX nano- and micro-particles. Particularly, we focus on nanoprecipitation and single emulsion, which are conventionally used methodologies but recently attract more attention with the development of microfluidics. Specific examples of drug-loaded Ac-DEX microparticles and NPs are summarized in Table 1, in terms of their preparation method, physical characteristics and drug loading efficiency. For other Ac-DEX constructs, such as scaffolds, microconfetti and nanofibers, we refer the reader to the review from Bachelder *et al.*[10]

Nanoprecipitation

Nanoprecipitation describes the bottom-up formation of NPs when the polymer solution encounters an antisolvent, or experiences a variation in pH and salt concentration.[51] The process of nanoprecipitation follows 4 distinct steps, namely, induction of a supersaturation condition, nucleation, rapid decrease in the supersaturation blocking further nucleation, and growth on the surface of the nuclei by deposition of monomers.[52] A deeper analysis of nanoprecipitation mechanisms can be found elsewhere.[52,53]

Conventional nanoprecipitation. Ac-DEX NPs can be produced in a conventional nanoprecipitation setup, *i.e.*, adding Ac-DEX organic solution to the miscible aqueous antisolvent under rapid magnetic stirring. Shkodra-Pula *et al.* dissolved Ac-DEX in acetone and controlled the addition of the polymer solution into the antisolvent (40 mL of 0.3% polyvinyl alcohol (PVA) aqueous solution) using a syringe pump to ensure a constant flow rate.[35] Solvent evaporation (acetone) was achieved by stirring for 24 h in a fume hood. The particles were then rinsed in ultrapure water to remove both residues of organic solvent and the PVA. Importantly, in order to prevent the pH-dependent degradation of the polymer, triethylamine was added to the water to increase the pH. The average size of the empty Ac-DEX particles after rinsing is 210 nm, with a PDI of 0.17. The size of the particles decreased when the particles were loaded with drugs and fluorescent probes to 163 nm. Furthermore, the particles were lyophilized and redispersed in ultrapure water. The average size remained constant (211 nm *vs.* 210 nm before lyophilization). However, the PDI increased from 0.17 to 0.26. These NPs were developed for the delivery of BRP-187, a molecule with anti-inflammatory effect. The loading degree achieved was on average 1.7%, with an average encapsulation efficiency of 59–67%.

Conventional nanoprecipitation can be employed also in the formulation of more complex core–shell NPs. For example, Kong *et al.* combined core calcium carbonate particles with a shell of Ac-DEX.[36] The core–shell particles were prepared by sequential nanoprecipitation steps: the core calcium carbonate

Table 1 The production methods, loading degree (LD), encapsulation efficiency (EE), and physical characteristics of drug loaded Ac-DEX-based particles

Production method	Drug	Polymer	Loading efficiency		Size	PDI	ζ-Potential (mV)	Ref.
			LD%	EE%				
Conventional nanoprecipitation	BRP-187	Ac-DEX	1.7%	59–67%	163 nm	0.26	−24	35
	Doxorubicin tanespimycin and afatinib[a]	Ac-DEX	—	Doxorubicin (75–86%), tanespimycin (up to 70%)	223 nm	0.33	ca. −20	36
Nanoprecipitation in microfluidics	Sorafenib	Ac-DEX	1–5%	—	350 nm	<0.1	−46.3	37
	Paclitaxel					<0.1		
	Methotrexate[a]		Up to 4.5%					
	XMU-MP-1[a]	Ac-DEX	7.8%	—	332 nm	0.11	−31.4	38
	Budesonide	Endosomolytic polymer grafted Ac-DEX	1.9%	—	190 nm	0.11	—	39
	Asiatic acid	Endosomolytic polymer grafted Ac-DEX	3.9%	80.7%	231 nm	0.16	—	28
Conventional single emulsion	Sorafenib[b]	SpAcDEX	58.5%	—	233 nm	ca. 0.2	42	40
	CHIR99021 and SB431542	SpAcDEX	CHIR99021 (1.25%), SB203580 (1.99%)[c]	CHIR99021 (40.6%), SB203580 (38.3%)[c]	ca. 360 nm	0.2	35	41
	CHIR99021 and SB203580	Putrescein-AcDEX	CHIR99021 (0.97%), SB203580 (1.67%)[c]	CHIR99021 (33.08%), SB203580 (25.29%)[c]	ca. 300 nm	0.2	35	23
	AR-12	Ace-DEX	—	31.5–80.7%[d]	250–260 nm[d]	—	—	42
Single emulsion in microfluidics	Sorafenib and celecoxib	Ac-DEX	0.5–4.2%[e]	85–97%[e]	5.3–6.8 μm[e]	—	—	43
Double emulsion	Granulocyte macrophage colony stimulating factor (GMCSF) and Nutlin-3a	SpAcDEX	—	GMCSF (31%), Nutlin-3a (88%)	350 nm	0.23	47.1	44
	Ovalbumin	Ac-DEX	Up to 7.4%	—	100–400 nm	—	—	11
	Anti-luciferase siRNA	SpAcDEX	76–98%	—	180–230 nm	—	9–19	19
	Rapamycin and pancreatic peptide P31	Ace-DEX	Rapamycin (0.9%), P31 (1.0%)	Rapamycin (90.3%), P31 (51.5%)	666 nm	—	—	14
	Immunodominant peptide (MOG) and dexamethasone	Ac-DEX	MOG (0.48%), dexamethasone (0.14%)	MOG (21.8%), dexamethasone (1.5%)	<1 μm	—	—	45
Spray drying	Paclitaxel	Ac-DEX	3.04%	71%	ca. 2 μm	—	—	46
	Curcumin	Ac-DEX	0.07–0.40%[f]	54–88%[f]	1.5–7.4 μm[f]	—	—	47
Electrospray	Resiquimod	Ac-DEX	Up to 0.54%	Up to 60%	1.3 μm	—	—	48
	3′3′-cGAMP (cGAMP) and resiquimod[g]	Ace-DEX	cGAMP (0.83%), resiquimod (0.075%)	cGAMP (83%), resiquimod (75%)	—	—	—	49
	Lapatinib and paclitaxel[h]	Ac-DEX, PLGA	Lapatinib (1.22–1.29%), paclitaxel (0.61–0.71%)	22–28%	ca. 160 nm	—	—	50

[a] The drugs were first loaded in core particles and then encapsulated in an Ac-DEX shell. [b] The drugs were precipitated on microfluidics as nanocrystals first and prepared in a sequential microfluidic nanoprecipitation. [c] The drug loading was quantified after particle functionalization with the peptides. [d] Tailorable, depending on the organic solvent used. [e] Tailorable, depending on the initial concentration of the polymer. [f] Tailorable, depending on the weight ratio of drug loaded NP and the feed concentration. [g] Coaxial electrospray setting. [h] Electrospray cojetting setup with two capillaries in parallel.

particles were precipitated by mixing a solution of CaCl₂ with a solution of K₂CO₃. Ac-DEX was precipitated on the particles by adding an ethanol solution of the polymer to the solution containing the calcium carbonate particles. Finally, the particles were isolated by centrifugation. The core presented a diameter of ca. 104 nm, while the coated particles increased the size to ca. 189 nm. Furthermore, the PDI increased from 0.17 for the calcium carbonate to 0.33 after coating with Ac-DEX. This complex system can load gold nanorods, small molecular drugs (doxorubicin) and antibodies, combining imaging functionalities and photothermal therapy with the delivery of drugs. The average encapsulation efficiency varied between 76 and 80% for doxorubicin.

Microfluidics nanoprecipitation. Despite the successful particle fabrication reported in conventional nanoprecipitation, the mixing times achieved in a vial under magnetic stirring are relatively long, leading to inhomogeneous deposition of polymer on the nuclei and agglomeration.[54] The resulted particles may have polydispersed size distributions, as well as batch-to-batch variations.[52,54–56] In contrast, microfluidic technology can accelerate solvent mixing in miniaturized capillary networks.[57–59] The superfast mass transfer allows for a controlled and reproducible formulation of polymer particles, up to 700 g per day from a single device.[54,60]

Santos' lab has developed glass-capillary based microfluidic chips in a co-flow configuration for Ac-DEX NP production by nanoprecipitation (Fig. 2a). Ac-DEX polymer was dissolved in the organic solvent pumped as the outer fluid, while the aqueous antisolvent was pumped as the inner fluid. By fast mixing the outer and inner fluids, particles produced by nanoprecipitation in microfluidics are smaller with a more homogeneous population compared to the bulk ones (Fig. 2b and c).[54] The key parameters affecting the final size and polydispersity (PDI) of Ac-DEX NPs include the choice of organic solvents, the polymer concentration,
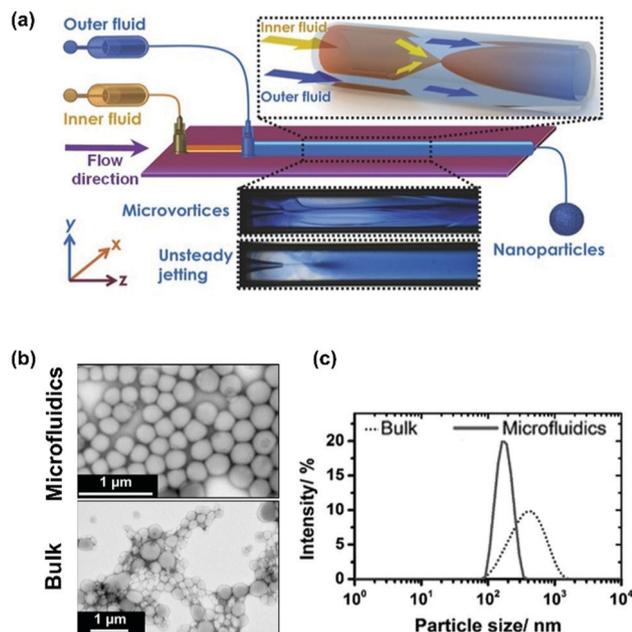
Fig. 2 Nanoprecipitation of Ac-DEX in microfluidics. (a) Scheme of glass capillary microfluidics nanoprecipitation setup. Microscope images of microvortex or unsteady jetting nanoprecipitation regimens. (b) The transmission electron microscopy (TEM) images of Ac-DEX NPs made by bulk and nanoprecipitation methods. (c) The dynamic light scattering distribution profile of Ac-DEX NPs made by bulk and nanoprecipitation methods. Modified and reproduced from ref. 54, with permission from John Wiley and Sons, Copyright © 2015.

the flow rate of both the inner and the outer fluids, and the surfactants in the aqueous phase to stabilize the final particles. The factors prolonging the mixing time (*i.e.*, higher viscosity of the organic solvent, higher polymer concentration, slower flow rate) often lead to an increase in the particle size and PDI. For instance, an increase in the viscosity of the organic polymer solution of the particle size and PDI results in moderate increase when changing from acetone through acetonitrile, methanol and ethanol, to then sharply increase when dimethyl sulfoxide was used.[54] Likewise, using PVA as the aqueous stabilizer increases the size of the particles due to the higher viscosity imparted from the surfactant to the solution, prolonging the mixing time.[54]

In addition to solid Ac-DEX NPs, microfluidic nanoprecipitation also enables the facile production of core/shell structures where various core particles are encapsulated within a layer of Ac-DEX matrix.[37–40,60] In a typical setting, the core particles are suspended in an Ac-DEX-dissolved organic solution, and subsequently precipitated in the aqueous antisolvent (Fig. 3a and b). Key parameters to evaluate when formulating these core/shell structures are the organic solvent, to be chosen as the best compromise between the solubility of the polymer and the stability of the core particle (*e.g.*, porous silicon is highly stable in ethanol, where Ac-DEX is soluble).[37,61] Furthermore, the choice of the surfactant depends on the size of the core particle and the desired size for the Ac-DEX shell (*e.g.*, when using porous silicon particles with dimension *ca.* 170 nm, PVA can be a suitable surfactant because it results in bigger Ac-DEX particles).[37,61]

In a more complex setup, different core NPs can be included within the shell of Ac-DEX. For example, porous silicon NPs and gold NPs were coated by nanoprecipitation in Ac-DEX matrix.[38] Ac-DEX derivatives, such as spermine-conjugated Ac-DEX (SpAcDEX) and Ac-DEX grafted polymers, have also been produced both as solid NPs and as core/shell structured nanocomposites on similar microfluidic nanoprecipitation platforms.[28,39,40,60]

When core/shell particles are prepared by nanoprecipitation, the therapeutic payloads can be loaded within Ac-DEX shell, or as the core (*e.g.*, drug nanocrystals), or pre-loaded within the porous core particles. Those payloads with similar solubility to Ac-DEX (*e.g.*, budesonide, paclitaxel, rifaximin, sorafenib)[37,39] can be dissolved together with Ac-DEX in the organic phase, and co-precipitated in the aqueous antisolvent (Fig. 3a). The loading degree can be quite easily tailored by adjusting the initial drug concentration(*e.g.*, for sorafenib and paclitaxel in the same formulation, their loading degree was tailored to 5% each).[37] However, the loading degree is limited by the maximum solubility of the drug in the solvent of choice; as an example, budesonide solubility in ethanol is lower than in other solvents, such as dimethyl sulfoxide, resulting in a lower loading degree (1.9%).[39] If high loading degree is desired, the drugs can be formulated as nanocrystals first, and then encapsulated in SpAcDEX as core particles (Fig. 3c). In this case, the nanocrystal solution has to be saturated with the drug, as well as containing a small amount of antisolvent for the drug (water) to prevent dissolution of the nanocrystals. Compared with simply encapsulation in Ac-DEX matrix, the drug nanocrystals method significantly increased the loading degree from 4.6% to almost 58.4% for sorafenib, making the final particle an ultra-high drug carrier.[40]

On the contrary, for drugs that are either insoluble in the organic solvent of choice or are soluble in water (*e.g.*, XMU-MP-1, methotrexate), the encapsulation within core NPs can increase the loading degree (Fig. 3a).[37,38,56] When the drug is loaded in the core particle, the loading degree depends on the properties of the drug and core particle (*e.g.*, porosity, highest loading capacity in the core particle) and on the solubility of the drug both in the organic and aqueous phases. For example, methotrexate is less soluble in ethanol than water, thereby the highest loading degree achievable when directly added to the ethanol solution before nanoprecipitation was 0.1%.[37] However, methotrexate is quite highly loaded within porous silicon NPs (loading degree around 30%). To prevent the release of methotrexate from porous silicon particles during the nanoprecipitation process, Liu *et al.* saturated the organic solution with methotrexate.[37] This allows to achieve a maximum loading degree of 4.5% in the final formulation.[37]

Single emulsion

Single emulsions are systems constituted of two immiscible liquids, usually oil-in-water, which are then mixed to form oil droplets dispersed in water. Single emulsions can be produced by high energy methods, such as sonication, commonly employed at lab scale.[62] During sonication, the two layers (oil and water) are disrupted and mixed due to the high energy force applied to the system (*e.g.*, cavitation from sonication). This process is not
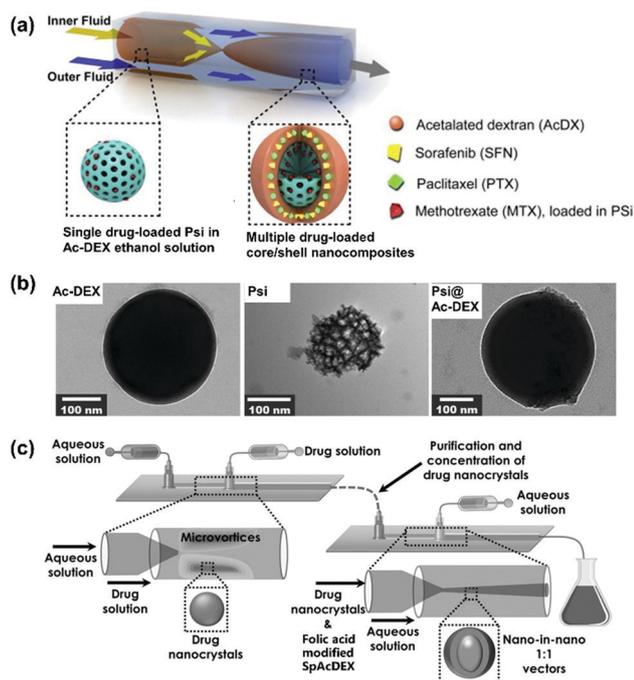
Fig. 3 Core/shell nanocomposites prepared by nanoprecipitation in microfluidics. (a) Scheme of porous silicon (Psi) encapsulated Ac-DEX core/shell structure produced by glass capillary microfluidics. Therapeutic payloads sorafenib and paclitaxel are encapsulated in the Ac-DEX matrix and methotrexate in the Psi core. (b) TEM pictures of Ac-DEX, Psi, and Psi encapsulated Ac-DEX (Psi@Ac-DEX) NPs. Adapted from ref. 37, with permission from Elsevier, Copyright © 2015. (c) Scheme of microfluidic platform for drug nanocrystals encapsulated folic acid modified SpAcDEX NP production. Reproduced from ref. 40, with permission from John Wiley and Sons, Copyright © 2017.

thermodynamically favourable because the formation of the emulsions increases the surface area, thereby a source of energy (e.g., sonication) has to be applied to the system to induce droplet breakdown.[52] Furthermore, the radius of the emulsions formed is directly related to the Laplace pressure, which measures the pressure difference between the inner and outer phase of the emulsion droplet.[63] Thereby, smaller emulsion droplets have higher Laplace pressure and require higher energy input to achieve droplet breakdown. Furthermore, emulsions are intrinsically unstable systems, thereby surfactants are needed to prevent the coalescence of the droplets one with the other. The mode of action of the surfactant is to interpose at the interface between the droplets and the continuous phase, preventing the coalescence via repulsion, increase in the viscosity of the solution, or increase in the solvation barrier.[52]

Conventional single emulsion. Conventional single emulsion techniques are often chosen in the production of Ac-DEX and derivatives micro- and nano-particles, particularly for Ac-DEX with positively charged modifications (SpAcDEX and Putrescein-conjugated Ac-DEX).[22,23,41] The polymer is dissolved in the organic phase (e.g., dichloromethane) before adding the aqueous phase containing the surfactant (e.g., PVA) and formation of the emulsion by homogenizer or high intensity sonication.[41,64] The careful optimization of the volumes of dispersed and continuous phase,

intensity and duration of the sonication and the temperature of the emulsion allow to achieve particles with size ca. 250 nm and quite narrow PDI values around 0.2 both for SpAcDEX and Putrescein functionalized Ac-DEX NPs.[23,41]

Single emulsion is usually suitable for the encapsulation of hydrophobic drugs with high solubility in the organic solvent chosen and low solubility in the aqueous continuous phase. The encapsulation efficiency and loading degree are dependent on the technique used to obtain the single emulsions and on the organic solvent chosen. The drugs chosen, CHIR99021, SB431542 and SB203580, are soluble in dichloromethane and are encapsulated within SpAcDEX and Putrescein NPs with an average loading degree between 0.97 and 1.99% and encapsulation efficiency up to 40.6%.[23,41] In another example, the encapsulation efficiency of AR-12 was increased from 31.5% to 80% when changing the solvent from dichloromethane to ethyl acetate, highlighting the impact of the solubility of the chosen drug in the organic solvent as the key factor to increase the encapsulation efficiency.[42] The change in the solvent did not alter the size of the obtained particles, with an average size of 255 nm for the particles prepared with dichloromethane and 260 nm for the particles prepared from ethyl acetate.

Microfluidics single emulsion. Although the size of particles and drug loading in conventional single emulsion can be easily tuned by adjusting the emulsifying parameters in a small lab scale, they become more problematic when scaling up to pilot and industrial size productions. A solution to improve the control over the emulsification is provided by microfluidics. The high degree of control achieved within a microfluidics system allows for the production of emulsions with precise dimensions and high homogeneity.[52] In single emulsion microfluidics, the polymer is dissolved in the organic phase in one channel, while the aqueous phase containing the surfactant in another. The emulsion is formed when the flow of organic solution is broken in T-junctions or at the tip of glass capillaries, by the accumulated pressure (T-junction) or by the shear stress determined by the flow of the aqueous solution. For a deeper discussion about single emulsion in microfluidics, we invite the reader to consult the review from Liu et al.[53]

We used glass capillary microfluidics in a flow-focusing configuration in the production of Ac-DEX microspheres (Fig. 4a). By dissolving the polymer in ethyl acetate and using poloxamer 407 as surfactant in the aqueous outer phase,[65] we managed to obtain solid microspheres. Furthermore, Santos' lab has developed a flow-focusing polydimethylsiloxane chip, which can produce hollow microspheres of Ac-DEX (Fig. 4b). Starting from single emulsion droplets produced in dripping regimen, we achieved high degree of control over the dimensions of the emulsion droplets.[43] We have carefully chose the organic solvent, dimethyl carbonate, to avoid swelling in the chip, as well as considering its favourable environmental and low toxicity properties when compared to other organic solvents. After formation, the droplets were left in the collection vessel with a large volumes of aqueous phase to facilitate organic solvent removal.[43,65] We found that the organic solvent diffusion from the droplets to the outer aqueous phase is responsible for the peculiar hollow microparticles (Fig. 4b; SEM image); during the

Feature Article

exchange process, the polymer is precipitating in a shell and effectively entrapping the residual organic solvent inside. Gravity and tensions forces at the interfaces determine the accumulation of the solvent on one side of the microparticles, increasing the pressure, until the entrapped solvent breaks the thin polymeric layer, escaping in the outer solution, leaving a hollow cavity in the microparticle.[43]

The concentration of the polymer in the dispersed phase marginally influences the final size of the particles, particularly in the case of hollow microspheres, whereas an increase in the concentration of the polymer from 1 to 100 mg mL^{-1} results into an increase in the size from 2.7 to 6.8 μm (Fig. 4c).[43] However, the increase in the size is paired with a decrease in the coefficient of variation between the microparticles (Fig. 4c), explained by the authors through the different thickness of the microsphere walls inducing deformation. The use of microfluidics allows for high encapsulation efficiency (96–97%), particularly when using high concentrations of polymer, where the drug can be entrapped in more polymeric matrix.[43] However, the presence of high amounts of polymeric matrix in the final particles is
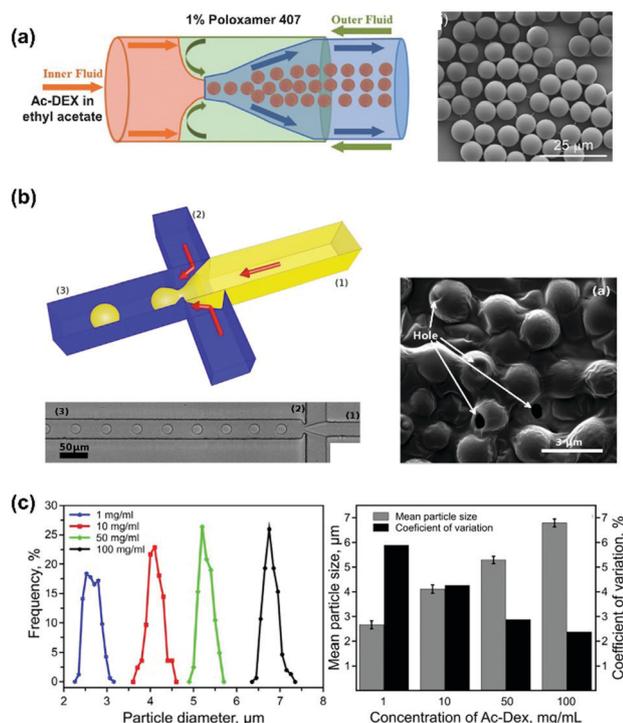

Fig. 4 Ac-DEX microparticles prepared by single emulsion methods in microfluidics. (a) The scheme of a flow-focusing glass-capillary based microfluidic device, and the scanning electron microscopy (SEM) image of the particles produced. Reproduced from ref. 65, with permission from John Wiley and Sons, Copyright © 2018. (b) The scheme and the corresponding microscopy image of a flow-focusing polydimethylsiloxane microfluidic chip for hollow Ac-DEX particle production: 1 indicates the inner fluid, and 2 the outer fluid and 3 the channel transferring the emulsions to the collection fluid. The inset is the SEM image of the particles produced, with arrows highlighting the holes. (c) The size distribution, mean size and coefficient of variation of Ac-DEX particles produced by the microfluidic chip in (b), using different polymer concentrations. Reproduced from ref. 43, with permission from American Chemical Society, Copyright © 2015.

responsible for the very low loading degree achieved (0.5%). The use of polymeric solutions with lower polymer concentration has lower encapsulation efficiency, but also lower polymeric mass, thereby presenting a final higher loading degree.[43]

Double emulsion

Double emulsions are formed by a primary emulsion encapsulated within a secondary emulsion droplet. In the pharmaceutical field, double emulsions are most often in the form of water in oil in water emulsions (w/o/w) and are suitable for the encapsulation of hydrophilic or sensitive payloads within water-insoluble polymers or for the formation of core/shell particles.[14,66] Double emulsions are conventionally produced by two distinct processes of emulsification; in the first one the molecule of interest is dissolved in an aqueous dispersed phase which is sonicated in the organic continuous phase. This organic phase constitutes the dispersed phase of the secondary emulsion process.[44] After the double emulsification, the particles are formed by solvent evaporation. Once again microfluidics offers an excellent degree of control over the emulsification process, with the possibility of controlling the number of primary emulsion droplets contained in each secondary emulsion droplet.[52] Nevertheless, to the best of our knowledge, no study has formulated microparticles of Ac-DEX or derivatives via microfluidics double emulsion technique.

Ac-DEX-based NPs produced by conventional double emulsion result into particles characterized by a size of ca. 270 nm with 0.5 wt% ovalbumin loaded.[11] The encapsulation efficiency of ovalbumin remained to be almost 100% at feed values up to 40 μg of protein per mg of Ac-DEX.[11] In terms of RNA payloads, Ac-DEX only had minimal encapsulation (5% encapsulation efficiency), but when the polymeric matrix was changed for the cationic SpAcDEX, the particles showed > 90% encapsulation of siRNA due to the electrostatic interactions.[19] Furthermore, it is possible to co-load SpAcDEX with both hydrophobic drugs and hydrophilic macromolecules. For example, Bauleth-Ramos et al. incorporated the apoptotic drug Nutlin-3a (Nut3a) along with SpAcDEX in the organic phase, and the cytokine (granulocyte-macrophage colony-stimulating factor, GMCSF) in the aqueous phase, to achieve co-loaded NPs with encapsulation efficiencies of 88% for Nutlin-3a and 31% for GMCSF, respectively.[44] The encapsulation efficiency of double emulsion is, however, lower than for other methods (e.g., electrospray) due to loss of hydrophilic cargo in the aqueous outer solution.[49]

Spray drying

Spray drying is a technique that atomizes a solution of payloads and matrix is in small droplets in a chamber with a flow of hot gas.[67] The particles are formed following the transfer of the solvent into the gas, before colliding with the walls of the apparatus or being collected in cyclones or filters. The control over the physical parameters of the particles is given by the optimization of the atomization setup, the temperature of the gas and chamber, and the concentration of the atomized solute. The reviews from Poozesh et al. and Singh et al. provide a deeper focus on the spray drying process and its scalability in the pharmaceutical industry.[67,68]

Spray drying has been used to produce Ac-DEX aerosol micro-particles, particularly for pulmonary delivery applications.[46,47,69–72] The microscale dry power facilitated the delivery and deposition on the mucosal layer of the lung *via* inhalation.[47,72] Furthermore, this technique can be used combined with single emulsion or nanoprecipitation. Specifically, drug-loaded Ac-DEX NPs were prepared by conventional oil-in-water single emulsion or nanoprecipitation first, and then spray-dried with excipients (Fig. 5a).[47,70,73] For example, Torrico Guzmán et al. formulated paclitaxel loaded Ac-Dex NPs *via* single emulsion, and then spray-dried along with mannitol.[46] The paclitaxel loaded NPs were *ca.* 200 nm in size with low PDI (<0.15), and the final microparticles were *ca.* 2 μm. After re-dissolution of the microparticles, the paclitaxel loaded NPs had an increase in size to 271 nm with a higher PDI (0.33), indicating particle agglomeration during the spray drying. The surface potential decreased from −3.14 to −18.47 mV, due to the presence of mannitol. Almost all the NPs were loaded in the microparticles, making the final paclitaxel loading of 3.04 wt%. Compared with

other fabrication techniques, spray drying is a well-established pharmaceutical technique with scale-up production capability. It is suitable to produce micro-sized aerosol powders, with high encapsulation efficiency and low water contents for long-term storage. However, the elevated temperature during the drying may limit its application with temperature-sensitive payloads.

Electrospray

Similar to spray drying, electrospray also atomises droplets of volatile solution containing the payloads and the polymeric matrix into the air, but towards a solid or liquid collector with opposite charge.[74] The tuning of process-related parameters, including temperature, distance from the collector, flow rate, viscosity, charge, volatile solvent used, impact the physical characteristics of the obtained particles, particularly size and morphology. For a deeper analysis of electrospray as a promising technology for the production of drug carriers and vaccines, we refer the reader to the reviews from Steipel et al. and Nikolaou et al.[74,75]

Electrospray has been widely employed in the formulation of Ac-DEX nano- and micro-particles.[10,49,76] For example, Duong et al. systematically investigated the use of a single capillary electrospray device (Fig. 5b) to formulate Ac-DEX microparticles.[48] To avoid particle aggregation, Tween 80 (10% v/v) was blended with Ac-DEX in ethanol, along with the payload (Toll-Like receptor agonist resiquimod). Most particles showed almost spherical morphology with aspect ratios close to 1, but with rough surface after drying (Fig. 5b). Compared with conventional oil-in-water single emulsion method, electrospray significantly increased the encapsulation efficiency by 10 times because it avoids the drug lost by diffusion to the aqueous phase.

Although single capillary electrospray device can encapsulate drugs soluble in the same organic solvent as polymers, it is difficult to encapsulate aqueous payloads even by preparing a water-in-oil emulsion before the spraying, because the payloads may get damaged with the high shear stress.[77] To solve this problem, Gallovic et al. developed a coaxial electrospray setup, which allows for the production of complex core–shell structures with sensitive payloads (Fig. 5c).[77] It shares some similarities to the double emulsion in microfluidics, with the coaxial alignment of two phases: polymer in the organic outer phase and aqueous protein payloads in the inner phase. The two immiscible phases encounter at the outlet of the concentric needles, and the solvent/water evaporate within sub-seconds. This coaxial electrospray platform has been successfully used to formulate Ace-Dex microparticles with different hydrophilic payloads, including recombinant anthrax protective antigen, cyclic dinucleotides, and poly I:C.[17,77,78] Furthermore, the hydrophobic payloads could be co-loaded in this setup, by simply mixing with Ac-DEX polymer in the organic phase.[49]

Apart from the single or multiaxial electrospray, the cojetting setup with two capillaries in parallel has been developed to fabricate poly lactic-*co*-glycolic acid (PLGA) and Ac-DEX hybrid bicompartmental NPs (Fig. 5d).[50] The NPs were less than 200 nm, much smaller than the ones formulated in the previous setups. However, a non-volatile solvent (dimethylformamide, 30% v/v)
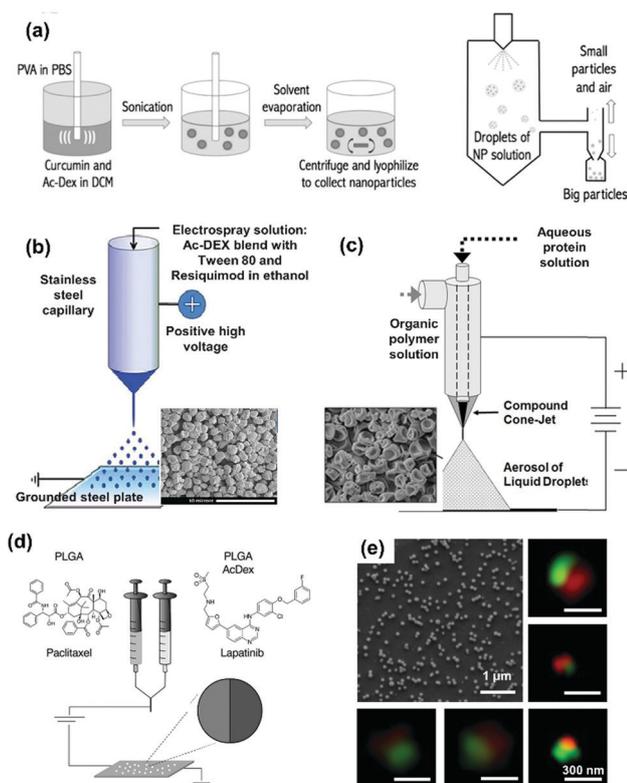

Fig. 5 (a) The scheme of spray drying combined with conventional oil-in-water single emulsion to make Ac-DEX microparticles. Reproduced from ref. 47, with permission from Elsevier, Copyright © 2017. (b) The scheme and the SEM images of Ac-DEX particles produced by a single capillary electrospray device. Reproduced from ref. 48, with permission from American Chemical Society, Copyright © 2013. (c) The scheme and the SEM images of Ace-DEX particles produced by a coaxial electrospray setup. Reproduced from ref. 77, with permission from John Wiley and Sons, Copyright © 2016. (d) The scheme of cojetting electrospray of bicompartmental Ac-DEX/PLGA NPs. (e) The SEM image and the super resolution structured illumination microscopy images of bicompartmental NPs loaded with different dyes. Reproduced from ref. 50, with permission from John Wiley and Sons, Copyright © 2020.

was used in this study, making an unfavourably long drying (3 weeks) to remove all the solvents. The resulted particles had two distinct compartments with different polymer compositions, as shown by the different dyes loaded in the super resolution structured illumination microscopy (Fig. 5e). The authors loaded a combination of two anti-cancer drugs (lapatinib and paclitaxel) in different compartments with a pre-determined ratio, which has the greatest synergistic effects. Such bicompartmental Janus particles allow for independent drug loading and release, thus making them versatile platforms for synergistic drug delivery.

Controlled release behaviour

The chemical modification of dextran to Ac-DEX and further derivatives introduces a feature fundamental for controlling the payload release, the pH-dependent degradation of the polymer. In this section, we will analyse the degradation behaviour based on the degree of substitution and how it influences the degradation of micro- and nano-particles. Finally, we will present alternative stimuli-responsiveness other than pH.

As discussed in the synthesis section, the acetals groups on Ac-DEX are prone to hydrolysis, resulting in the polymeric particle degradation. The hydrolysis rate is pH-dependent, which means the polymers degrades faster at acidic pH than at neutral or slightly basic pH. The pH-dependent degradation of Ac-DEX and derivatives represents one of the attractive features of the polymer in drug delivery and immunotherapy. The faster degradation at pH 5.0 compared to pH 7.4 is desired to control the release of drugs intracellularly at endosomal level or in tissues presenting lower pH (e.g., cancer, infarction, intestinal inflammation).[37,39,41,56]

The most important parameter to control the degradation rate is the percentage of cyclic groups on the polymer, because the cyclic acetals degrade slower than acyclic ones, thus becoming the rate-limiting step.[11] The percentage of cyclic groups correlate well with the acetalation reaction time (Fig. 6a). Thus, by controlling the reaction time, it is possible to control the degradation half-life (Fig. 6b).

Another important parameter to determine the degradation rate is the molecular weight of dextran. In an initial study, Kauffman et al. prepared Ac-DEX with similar cyclic percentage, but with different molecular weights (10 kDa and 71 kDa). The particles prepared from 10 kDa Ac-DEX degraded reached complete degradation much faster than the ones made from 71 kDa Ac-DEX at pH 4.9, although the half-life of both polymers were similar (Fig. 6c).[64] After an initial fast degradation, the particles made by 71 kDa showed slower degradation rate afterwards, possibly due to the higher viscosity of the polymer.[64] In another study, Chen et al. systematically investigated the degradation profiles of Ace-DEX prepared from 4 different molecular weights (10, 71, 500, 2000 kDa) with three degrees of cyclic acetals (20, 40 and 60%).[79] For polymers with low coverage of cyclic acetals (20%), all displayed fast degradation at pH 5.0 (half-life 0.25 h) regardless of molecular weight. For those with medium cyclic acetal coverage (40%), the degradation half-life at
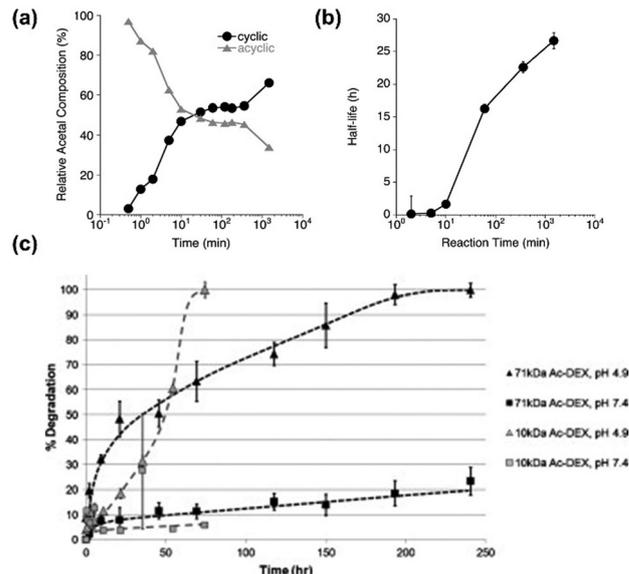

Fig. 6 The degradation of different Ac-DEX polymers. (a) The cyclic and acyclic acetal groups in the polymer composition plotted against reaction time. (b) The degradation half-life of AcDEX of different reaction times at pH 5.0. Reproduced from ref. 11, originally published by National Academy of Sciences, Copyright © 2009 National Academy of Sciences. (c) The degradation kinetics of Ac-DEX of 10 kDa and 71 kDa at pH 4.9 and 7.4. Reproduced from ref. 64, with permission from Elsevier, Copyright © 2012.

pH 5.0 is inversely related to the molecular weight of the polymer (larger polymers degrade faster). For those with 60% cyclic acetal coverage, the degradation half-lives were again similar for 10, 71 and 500 kDa (half-life ca. 21 h), consistent with the previous report.[64] Therefore, a careful choice of cyclic acetal coverage and a thoughtful combination of the most suitable molecular weight allow to obtain Ac-DEX polymers with the desired degradation profile for the chosen application.

Although polymer degradation is the most critical factor affecting the release kinetics, other factors, such as the production method and the type of particle (solid NP vs. core/shell composite), also have an impact on the overall release performance. Solid Ac-DEX NPs prepared by single emulsion often display a burst release derived from drug adsorbed on the surface of the particle or encapsulated within the most external layers of the particle in acidic pH.[41] Interestingly, regardless of the drug loaded, the release profile of Ac-DEX at pH 7.4 display the release of ca. 20% of the encapsulated payload when using Ac-DEX 10 kDa and 5 h reaction time.[39,41] The release of payloads within the core particles is influenced by the type of core particle; porous silicon NPs rapidly release their payload, thereby the release of methotrexate is influenced by the degradation of the polymer and not by the presence of the core particle.[37] The same is valid also when the drug itself represents the core particle; the release of sorafenib nanocrystals is dependent on the degradation of the polymer, which prolongs the release when compared to nanocrystals alone.[40]

Although the main release mechanism for Ac-DEX and its derivatives is pH-dependent as described above, recent innovative designs have allowed degradation of the polymer and release in

response to other stimuli. For example, particles degradation can be sensitive to environmental glucose by encapsulating within the particles glucose oxidase, which upon reaction with glucose, generates gluconic acid and decreases the pH, resulting into the degradation of Ac-DEX.[80,81] Another inspiring example is the UV-responsive degradation of Ac-DEX particles, by incorporating light-sensitive photoacidic generators (2-(4-methoxystyryl)-4,6-bis(trichloromethyl)-1,3,5-triazine).[82] In this case, the local acidity can be achieved through the introduction of UV-light, reducing the dependence of the degradation from the *in situ* pH conditions.[82] High power near-infrared laser can also induce drug release from Ac-DEX particles, due to the thermal effects rather than particle degradation.[83]

Biomedical applications

The versatility of Ac-DEX in the production of micro- and nano-structures, combined with the possibility to tune the degradation profile based on the molecular weight of the polymer and the reaction conditions, results into a wide range of therapeutic applications, from vaccines for infective disorders to cancer vaccines, cancer treatment, immunomodulation for autoimmune diseases, and applications in the treatment of cardiovascular diseases and infectious diseases. Here, we will present selected applications in the different therapeutic categories.

Vaccination against infectious diseases

Modern vaccines are often composed of subunits, pieces of proteins, or nuclei acids coding for pathogen proteins. These vaccines are generally safer than living or attenuated vaccines because there is no risk of the pathogen reactivating. However, the downside of these highly purified vaccines is their efficacy; the peptidic antigens administered as such are not able to induce a proinflammatory immune response and often require the use of adjuvants with optimal efficacy achieved upon co-admnistration of antigens and adjuvants.[84]

The first therapeutic application of Ac-DEX reported is as vehicle for vaccines.[11] In particular, in the first studies, the effect of different reaction times on effective antigen presenting cell (APC) maturation, was evaluated and quantified as amount of major histocompatibility complex (MHC) I and II expressed on the cells (Fig. 7a).[11] Ac-DEX (reaction time 10 min) showed highest MHC I and II presentation over crosslinked polyacrylamide (PA), PLGA and iron oxide NPs.[11] Interestingly, Ac-DEX microparticles display different mechanisms of activation of APCs depending on the reaction time; particles made from Ac-DEX reacted for 10 min are independent from transporter associated with antigen processing, underlying the presence of multiple mechanisms involved, including osmotic disruption of lysosomes.[11]

Furthermore, Ac-DEX has been used as carriers for various adjuvants. Several studies have demonstrated the possibility to encapsulate both small molecules as imiquimod and STING agonists and larger molecules like CpG and polyinosinic:polycytidylic acid within Ac-DEX micro- and nano-particles
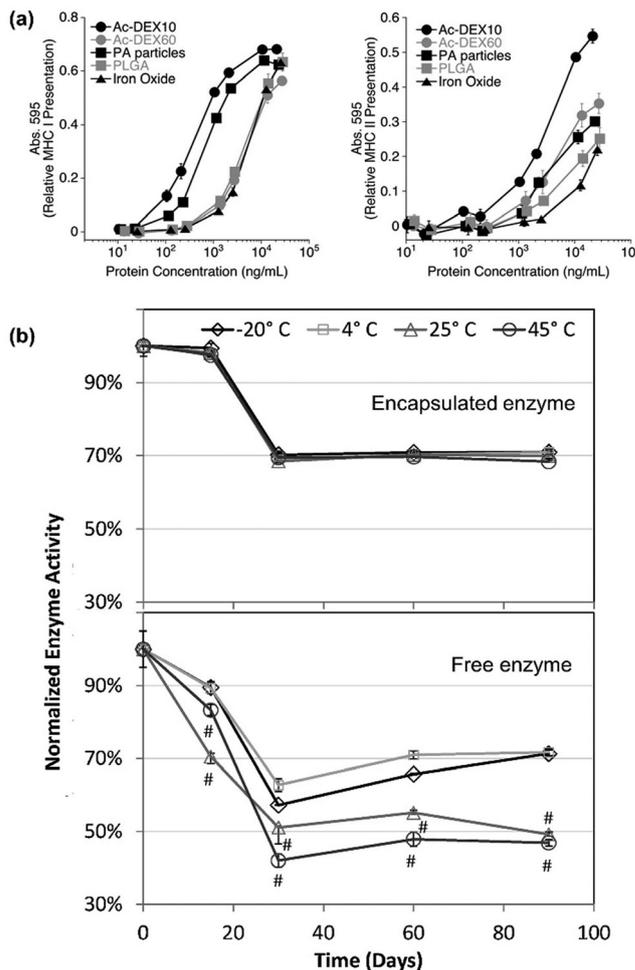

Fig. 7 Ac-DEX-based vaccines. (a) Efficacy in promoting the presentation of antigen on MHC I and II. The efficacy of Ac-DEX NPs synthesized with different acetalation reaction time (10 min and 60 min, AcDEX10 and AcDEX60, respectively), are compared with common vaccine delivery vehicles, *i.e.*, crosslinked polyacrylamide (PA), poly lactic-*co*-glycolic acid (PLGA) and iron oxide NPs. Reproduced from ref. 11, originally published by National Academy of Sciences, Copyright © 2009 National Academy of Sciences. (b) Storage stability over time of horseradish peroxidase-loaded Ac-DEX particles within (−20 °C and 4 °C) and outside (25 °C and 45 °C) cold chain. Up, the stability of enzyme in particles produces by homogenization; down, the stability of the free enzyme. Reproduced from ref. 87, with permission from Elsevier, Copyright © 2012.

produced by electrospray and single emulsion.[49,85,86] Ac-DEX can also encapsulate NP adjuvant, which induced the activation of antigen presenting cells, such as thermally oxidized porous silicon.[61]

Another fundamental characteristic of vaccines is their storage temperature. The possibility to store the vaccine formulation in fridge or at room temperature highly facilitates the logistics and the distribution, important in case of a pandemic. Ac-DEX microparticles can protect biological payloads, such as horseradish peroxidase, at room temperature (25 °C) and higher temperatures (45 °C), maintaining 70% of the initial activity independently from the storage conditions (Fig. 7b).[87] Furthermore, Ac-DEX vaccine formulations can tolerate γ-rays irradiation as sterilization method.[78]

Given the favourable properties of Ac-DEX particles as vaccine carriers, a wide array of formulations has been investigated for the prevention of infectious diseases. The production of Ac-DEX microparticles with electrospray can maintain the correct structure of the recombinant antigen, when compared to the conventional emulsion technologies. The resulted vaccine induced a titer of antibodies comparable to conventional alum vaccines and protecting mice against challenge with *Bacillus anthracis*.[77,88] At the same time, the modulation of the degradation properties of the polymer result into a flexible and versatile platform for a universal vaccine against influenza with differences in the protective efficacy *in vivo*.[89] This, combined with the use of STING agonists as adjuvants, can increase both the humoral and cellular immunity against influenza virus, greatly improving the efficacy of the vaccine *in vivo*.[78] Recently, this platform has been investigated also in the challenging field of malaria vaccines; the adsorption of the antigenic protein on the surface of Ac-DEX microparticles skewed the immune response towards a Th1 type, needed in the fight against an intracellular pathogen, more than conventional alum formulations.[90]

Overall, acetalated dextran is an optimal candidate for the formulation of vaccines for infectious diseases, particularly in the case of intracellular pathogens, where a cellular response is needed and is not easily achieved with conventional vaccine formulations. The protection of the payload from temperature and sterilizing ionization are of extreme interest for the further translation of these platforms towards clinical use.

Tolerogenic vaccines for autoimmune diseases

Autoimmune diseases are characterized by the activation of humoral or cellular immune response against healthy cells of the human body, from red blood cells to β cells in the pancreas, to myelin-producing cells in the brain.[91] Tolerogenic vaccines can induce antigen-specific tolerance targeting the autoantigens associated with each disease.[92] Tolerogenic vaccines and other treatments for autoimmune diseases can be associated with systemic immunosuppression with potential side effects.[93] Micro- and nano-particles allow a localized therapy, contributing to the reduction of the systemic side effects.[93]

Tolerogenic particulate vaccines are usually composed of the disease specific autoantigen and an immunosuppressant co-loaded within the same particle. Ainslie's group evaluated the potential of Ac-DEX and Ace-DEX microparticles as tolerogenic vaccines.[14,45,64,94] Rapamycin is often chosen as an immunosuppressant, combined with different disease-specific antigens. Kauffman *et al.* characterized the parameters influencing the physicochemical properties of rapamycin-loaded Ac-DEX particles prepared by single emulsion, with the overall aim to increase the encapsulation efficiency of rapamycin while slowing the release profile.[64] The loading of rapamycin within Ac-DEX particles reduces the inflammatory response in raw macrophages at levels comparable to the free drug. Chen *et al.* prepared ovalbumin and rapamycin-loaded Ace-DEX microparticles by double emulsion.[94] These particles had a pronounced anti-inflammatory effect *in vitro*, and protected mice from the development of encephalomyelitis, the murine model

for multiple sclerosis, in an antigen-dependent manner. Rapamycin-loaded Ace-DEX particles are extremely versatile platforms for tolerogenic vaccination: by changing the disease-specific autoantigen, the same platform can be successfully translated to the prevention of type 1 diabetes *in vivo*, with only one mouse presenting high levels of blood glucose and developing diabetes.[14]

Alternatively to rapamycin, Ac-DEX-based tolerogenic vaccines can be also formulated with dexamethasone.[45] In this work, myelin oligodendrocyte glycoprotein was chosen as a disease-specific antigen instead of ovalbumin. A treatment plan with three subcutaneous administration of the particles, with an interval of three days between each administration, can significantly improve the clinical score in encephalomyelitis mice.

Cancer vaccines

Cancer immunotherapy has contributed to a revolution in the treatment of several types of cancer. This treatment involves the patient's own immune system to identify and destroy cancer cells.[84] As in the case of infectious diseases, the immune system needs antigens to correctly identify cancer cells. At the same time, cancer can be assimilated to an intracellular pathogen, requiring the priming of a Th1 skewed response with a preponderant cellular immunity.[84] Thereby, cancer vaccines needs to present tumour associated antigens with systems able to induce cellular immunity. As discussed above, the use of Ac-DEX-based particulate systems is promoting the presentation of MHC-I and the priming of lymphocytes, rendering it an optimal platform for the development of cancer vaccines.

To this end, Watkins-Schulz *et al.* focused on the modification of Ace-DEX microparticles with STING agonist, evaluating both the mode of action and the antitumour efficacy in melanoma and breast cancer (Fig. 8a).[17] Firstly, they confirmed that STING agonist 3′3′-cyclic GMP-AMP (cGAMP) is the adjuvant promoting the highest activation of the immune system, compared with other adjuvants evaluated. Specifically, murine models of melanoma were injected with different adjuvant loaded in Ace-DEX microparticles. cGAMP-loaded particles (cGAMP MPs) prolonged the control over the tumor growth, with a statistically significant difference, compared to the other adjuvants (murabutide, imiquimod, poly I:C) loaded particles and blank particles. Moreover, compared with free cGAMP, cGAMP MPs increase the efficacy of the adjuvant (by at least 2-fold increase in the secretion of interferon-β, tumor necrosis factor, and interleukin 6), and activate both cytotoxic T cells and natural killer (NK)-cells. This suggests the cGAMP loaded Ace-DEX particles can generate robust innate and adaptive anticancer immune responses.

The next step in the development of a successful cancer vaccine is the choice of antigens. Potent cancer antigens are antigens expressed mainly or only from the majority of cells within the tumour. Furthermore, each patient will have an individual antigenic signature, making the case for personalized cancer vaccines. The techniques routinely employed for the isolation of epitopes and for the evaluation of the ligandome are still costly and time consuming.[95] The use of isolated cancer cell membranes as sources of antigens offer a convenient and fast alternative for present-day cancer vaccines.[84]
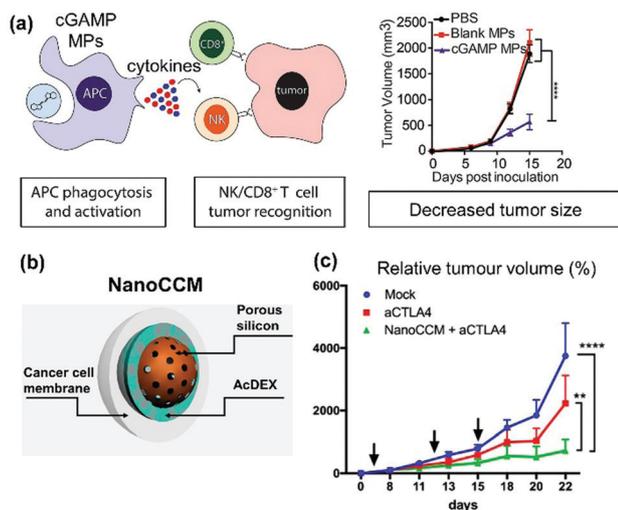
Fig. 8 Acetalated dextran particles as cancer vaccines. (a) Schematic of the mechanism of action of STING-agonist loaded Ace-DEX microparticles after *in vivo* administration, and tumour growth curve of B16.F10 melanoma tumour after intratumoral administration of the cGAMP adjuvant-loaded Ac-DEX particles. Reproduced from ref. 17, with permission from Elsevier, Copyright © 2019. (b) Schematic of cancer cell membrane wrapped core/shell porous silicon@Ac-DEX particles. (c) Tumour growth curve of B16.OVA melanoma after administration of immune checkpoint inhibitor (aCTLA-4) or a combo treatment of immune checkpoint inhibitor and NanoCCM cancer vaccine. Reproduced from ref. 96, with permission from American Chemical Society, Copyright © 2019.

This antigenic source (in particular cell membranes derived either from breast cancer cells or from melanoma) wrapped a core/shell structure composed of porous silicon NPs embedded within an Ac-DEX matrix (NanoCCM, Fig. 8b).[61,96] The combination of antigen and adjuvant efficiently activated APCs both *in vitro* and *in vivo*. Furthermore, the peritumoural administration of the final system combined the efficacy of both Ac-DEX particles and cell membranes.[96] Finally, this type of cancer vaccine improves the therapeutic efficacy of immune checkpoint inhibitors (the standard of care for melanoma) when used in combination by priming an antitumour immune response which is then amplified by the immune checkpoint inhibitors such as aCTLA4 (Fig. 8c).[96]

Cancer therapy

In addition to the cancer vaccines, Ac-DEX-based anti-tumour therapeutic delivery systems have been developed to enhance the efficacy of chemotherapy, photodynamic therapy and the emerging chemo-immunotherapy. In these delivery systems, Ac-DEX or its derivative polymers are mostly formulated as NPs (100–500 nm), and deliver drugs to tumour *via* passive accumulation by the enhanced permeation and retention effect (EPR effect), or *via* active targeting by the conjugation of certain tumour-targeting ligands. Then, the pH-responsive degradation in the acidic tumour microenvironment triggers the drug release to eliminate cancer cells. Although the basis of EPR effect is not completely understood and still in dispute,[97–100] the Ac-DEX-based delivery systems have shown some promising results *in vivo*.[101,102] Below, we briefly introduce the application

of Ac-DEX-based delivery systems in different cancer therapies, and highlight some novel designs.

The delivery of chemotherapeutic drugs by Ac-DEX and its derivatives mostly focuses on the enhancing the solubility, bioavailability of the poorly soluble drugs and reducing the systemic side effects, compared with the free drugs alone. This concept was addressed by Dai *et al. via* the controlled delivery of a highly toxic anticancer drug (maytansinoid, denoted as AP3).[101] Compared with conventional chemotherapeutics, such as doxorubicin, AP3 displayed 100–10 000 times more potency.[103] However, AP3 alone did not show satisfactory *in vivo* tumour inhibition, due to the severe side effects and narrow therapeutic window. By encapsulation in the pH-responsive Ac-DEX NPs decorated by PEG on the surface, Dai *et al.* extended the half-life of the drug in the blood by 7 times, and achieved better tumour growth inhibition on xenograft models.[101] The systemic toxicity of AP3 encapsulated NPs towards major organs, such as heart, lung, liver, spleen, kidney and intestine was negligible, while free AP3 induced severe liver damage, confirmed by hematoxylin and eosin staining.[101] The overall results showed PEG-conjugated Ac-DEX carrier showed promising potential for the delivery of highly toxic drugs for antitumour therapy.

Another example of delivering toxic antitumour agents, is the core/shell structured prickly zinc-doped copper oxide NPs encapsulated in SpAcDEX, with 3-(cyclooctylamino)-2,5,6-trifluoro-4-[(2-hydroxyethyl)sulfonyl]benzenesulfonamide (VD1142) ligand conjugated on the surface (Fig. 9a).[104] As a result of the prickly nature of the zinc-doped copper oxide NPs, they were able to physical rupture the lipid membranes, thus showing high cytotoxicity.[104] By encapsulating in SpAcDEX, the biological stability and safety of the zinc-doped copper oxide NPs were improved.[104] Furthermore, the polymer coverage rendered the pH responsiveness to the system. After endocytic uptake, the acidic endosomal environment triggered the dissolution of SpAcDEX shell, exposing the prickly NPs, which ruptured the endosomal membrane and escape to cytoplasm, as shown in Fig. 9b.[104] These prickly NPs underwent disintegration during the endosomal escape process, and the produced ultrasmall particles induced damaging effects toward the destruction of the cellular organelles, such as endoplasmic reticulum and mitochondria.[104] The VD1142 ligand on the surface endowed the system with the targeting of carbonic anhydrase IX, a transmembrane protein overexpressed in a wide variety of cancer tumours.[104] *In vitro* results suggest these VD1142 conjugated core/shell structured SpAcDEX NPs showed more toxicity towards MCF-7 breast cancer cells and doxorubicin-resistant MCF-7 than fibroblasts, probably due to the VD1142 targeting effects.[104] Despite the lack of *in vivo* validation, the nanocomposites, which induce physical intracellular damage and caspase-independent cell death, explored new ways for targeted cancer therapy.

Although toxic drugs or needle-like NPs can kill cancer cells, the incomplete removal of cancer cells and the recurrence is still a worrying issue. To better resolve this problem, the combination of chemotherapy with immunotherapy is proposed, which aims to stimulating the immune system to recognize tumour associated antigens released from the cancer cells killed by

chemotherapy. In a typical combined chemo-immunotherapy, the formulation incorporates both chemotherapy drugs, and immunostimulators, which facilitate to active or restore the immunity, similar to cancer vaccines described above.[105] Bauleth-Ramos et al. used SpAcDEX to make a nanocomposite for chemo-immunotherapy, by co-loading non-genotoxic molecule Nut3a, and an antigen presenting cell activating cytokine GMCSF.[44] It was found that the nanocomposites maintained the pH-responsive release of Nut3a to kill cancer cells, and endosomal escape behaviour, which was attributed to the "proton sponge" effect caused by the cationic amine groups from SpAcDEX.[44] An effective antitumour immune response was observed as a result of GMCSF presence in the system, a complementary effect to specific toxicity of Nut3a toward wild-type p53 cancer cells while avoiding toxicity in immune cells.[44] Upregulated expression of cell surface CD83 co-stimulatory marker, decreased secretion of IL-10, and enhanced level of IL-1β were the main immunostimulatory effects of the developed nanosystems for cancer chemo-immunotherapy.[44]

In addition to chemotherapeutic drugs or immunostimulators, Ac-DEX-derivative polymers can also be employed to deliver

Fig. 9 (a) Schematic illustration of the efficient targeting of cancer cells and the antiproliferative effect by the engineered Prickly@SpAcDEX–PEG–VD1142 particles fabricated by microfluidic encapsulation of Prickly NPs in SpAcDEX nanomatrix, and subsequently surface conjugated with PEG–VD1142. The endosomal escape and structural regulated nanopiercing of endoplasmic reticulum and mitochondria in cancer cells are also highlighted. (b) Up, the TEM images of Prickly particles and the final formulation Prickly@SpAcDEX–PEG–VD1142 particles. Down, the confocal images of the intracellular uptake and endosomal escape of Prickly NPs and Prickly@SpAcD–PEG–VD1142 in MCF-7 breast cancer cells under hypoxia conditions. The blue fluorescence represents VD1142; the green fluorescence represents the FITC-labelled particles and the red fluorescence represents Lysotracker, which stains the endo/lysosomes. White arrows indicate the green particles that did not overlay with blue and red. Reproduced from ref. 104, with permission from John Wiley and Sons, Copyright © 2017. (c) The schematic illustration of the Ac-DEX-based oxygen delivery system and the in vivo tumour oxygen level after the intravenous injection of Ac-DEX-oxygen nanobubbles, oxygen saturated PBS solution, and Ac-DEX-nitrogen nanobubbles as a control. Reproduced from ref. 109, with permission from American Chemical Society, Copyright © 2019.

photosensitizer for photodynamic cancer therapy. Butzbach et al. encapsulated 5,10,15,20-tetraphenyl-21H,23H-porphyrine (TPP) in folic acid functionalized SpAcDEX.[24] The folic acid conjugation on the NP surface enhanced the uptake by folic acid receptor α over-expressed HeLa-KB cells in vitro, despite the fact that SpAcDEX without folic acid conjugation also showed significant cellular uptake by non-specific binding.[24] The following irradiation by visible light (338 kJ m^{-2}, 15 min) caused pronounced photoinduced cytotoxic effects on HeLa-KB cells, even on the cells with short exposure to the NPs (1.5 h incubation).[24] This suggests the potency of photodynamic therapy, by selective targeting of folic acid receptor α over-expressed cancer cells using folic acid functionalized SpAcDEX NPs.

Another innovative application of Ac-DEX NPs, is to delivery oxygen for alleviation of tumour hypoxia, which is one of the main causes of cancer resistance to photodynamic therapy and radiotherapy.[106–108] Song et al.[109] prepared oxygen nanobubbles and enclosed them within pH-responsive Ac-DEX shells for the spontaneous generation of oxygen in response to a minor pH drop in the tumour microenvironment (Fig. 9c). The Ac-DEX shell was able to act as a barrier against gas dissolution in the blood circulation to efficiently deliver oxygen into the mild acidic tumour microenvironment in vivo (Fig. 9c), thus overcoming the hypoxia-induced resistance. Compared with well-known oxygen delivery agents, such as perfluorocarbon nanoemulsions, Ac-DEX oxygen delivery system avoids the premature oxygen release and the requirement of external stimuli (ultrasound activation).[109,110]
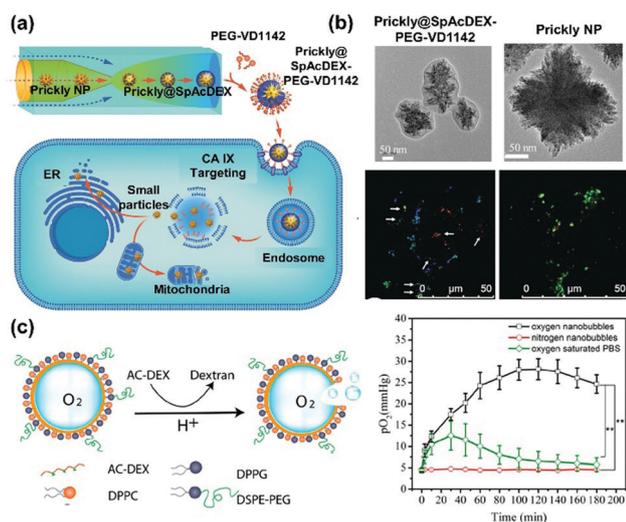
Cardiovascular diseases therapy

Cardiovascular diseases are currently a global burden with a high mortality rate due to the inability of the human adult heart to regenerate damaged cardiomyocytes and restore cardiac function.[111–113] Current therapies are mainly focusing on the alleviation of disease symptoms rather than changing the fate of cardiomyocytes, which indicates the necessity of novel therapeutic formulations. The emerging application of Ac-DEX[73,114,115] has brought new insights into the emerging of innovative treatment approaches through smart targeting strategies despite the challenges associated with the constant pumping of the heart and the restless massive exchange of blood.[116] For example, Santos' lab has developed PEG and atrial natriuretic peptide (ANP) surface-functionalized SpAcDEX NPs for direct reprogramming of fibroblasts into cardiomyocytes (Fig. 10a).[41] While PEG enhanced the colloidal stability and biocompatibility of the NPs (Fig. 10b), ANP enhanced the interaction of the NPs with cardiac cells due to the presence of natriuretic peptide receptors (NPR) on the cell membrane.[117,118] Here, we co-loaded SB431542 and CHIR99021, two poorly water-soluble drugs. CHIR99021 was able to stabilize β-catenin, and SB431542 prevented the translocation of Smad3 to the nucleus of myofibroblasts, two biological functions that promote heart regeneration. In general, this work showed the potential of Ac-DEX NPs for cardiac regeneration therapy via combined dual delivery and targeting of the damaged heart to efficiently reprogram fibroblasts into cardiomyocyte-like cells.
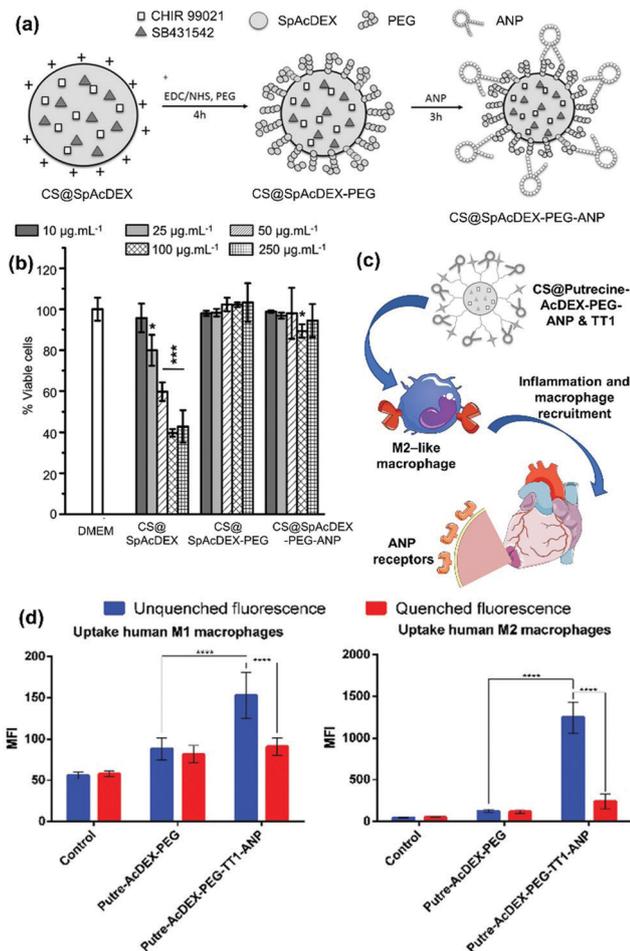
Fig. 10 (a) Illustration of the PEG and ANP stepwise functionalization of drug-loaded SpAcDEX prepared by an oil/water single emulsion method using crosslinking chemistry. (b) The cytotoxicity of drug loaded SpAcDEX, PEGylated SpAcDEX and the final formulation on cardiac nonmyocytes. The results are shown as the mean ± s.d. ($n \geq 3$). The levels of significance were set at probabilities of $*p < 0.05$, $**p < 0.01$, and $***p < 0.001$, compared with the cell medium-treated control. Reproduced from ref. 41, with permission from John Wiley and Sons, Copyright © 2018. (c) Illustration of ANP and TT1 dual-peptide functionalized Putricine conjugated Ac-DEX particles loaded with SB431542 and CHIR99021. The particles show high association with M2-like macrophages, and thus, suitable to "hitchhike" macrophages and target infarcted heart in the later stage of the inflammatory responses. (d) Quantitative cell uptake studies on human M1- and M2-like macrophages. Interactions between NPs and cells are represented as MFI values ± s.d. ($n = 3$). The significance levels of the differences were set at probabilities of $*p < 0.05$, $**p < 0.01$, and $***p < 0.001$, and $****p < 0.0001$. Reproduced from ref. 23, published by The Royal Society of Chemistry, under the Creative Commons Attribution-NonCommercial 3.0 Unported License.

Nevertheless, ANP, which was suggested for guiding NPs to accumulate in the infarcted heart, suffers from the expression of its receptor in other organs, such as lungs, kidneys, testes, brain, adipose tissue, vascular smooth muscle cells, and adrenal gland tissues.[119] To circumvent this drawback, Santos' lab further introduced dual-peptide functionalized Ac-DEX NPs for sequential targeting of macrophages and cardiac cells during myocardial infarction.[23] In this study, putrescine was

used for the modification of the polymer to provide desirable functional groups for further surface conjugations with peptides and to diminish the toxicity towards primary cardiomyocytes, which was reported with positively charged SpAcDEX NPs (Fig. 10c). CHIR99021 and SB203580 were loaded within the NPs for synergistic stimulation of cardiomyocyte proliferation,[120] and the surface of the nanocarrier was modified with TT1 and ANP, to endow them with heart targeting ability. TT1 peptide can bind to the mitochondrial chaperone protein p32, which is normally expressed on macrophages associated with atherosclerotic plaques.[121] Considering the obvious role of inflammation during infarction, TT1 was used to target macrophages that were migrated to the damaged heart tissue in order to improve the ANP mediated homing of the NPs in the infarcted heart.[23] The cellular studies demonstrated the NPs were more uptake on M2-like macrophages than M1 (Fig. 10d), indicating the suitability of the developed nanosystems for achieving the "hitchhike" effect and targeting of the infarcted heart in the later stage of the inflammatory responses. These studies were proof of concept investigations for the promotion of cardiac regeneration via Ac-DEX NPs, which may be extended to other nanoparticulate systems.

Infectious diseases therapy

There is currently a broad range of anti-infection compounds that are paramount to fight pathogens. Nevertheless, bacterial resistance to these molecules has become a major challenge worldwide due to their broad use and abuse, which result in the pathogen resistance and emergence of diseases that were under control for many years. This has prompted the development of nano- and micro-scale materials as alternative strategies to combat bacteria via their intrinsic killing effect or the delivery of antibacterial agents with the aim of improving their biological performance.[122,123] For example, one approach to overcome multidrug-resistant pathogens and kill intracellular infectious agents is through the loading of host-directed therapeutics (HDTs) within NPs for the targeting of host cells rather than the pathogen. However, most of HDTs agents can be toxic to the host cells and/or are hydrophobic with limited cellular internalization.

To cope with these challenges, Ace-DEX has been offered recently as a carrier for AR-12, a HDT agent, to improve its solubility and reduce its toxicity towards host cells.[13,42,124] In the reported works, intracellular drug concentration was increased in murine bone marrow-derived macrophages (BMDMs) and human monocyte-derived macrophages (hMDMs), when compared to free AR-12. Moreover, pH-responsive degradation kinetics of Ace-DEX particles allowed better control over the release of the antibacterial AR-12 agent in the intracellular site of action. This is crucial to kill facultative intracellular pathogens, such as Salmonella spp. and Francisella spp., which are challenging to treat due to their residence within intracellular vesicles and the cytosol.[124] In addition to the treatment of bacterial infection, Ace-DEX was also suggested to treat visceral leishmaniasis (VL), a disease caused by parasites of Leishmania sp., and to reduce the risk of its resistance due to the long treatment regimens with available therapeutics.[125] Similar to

above-discussed examples, AR-12 was loaded into Ace-DEX microparticles for the systemic treatment of VL, showing a significantly reduced load of the parasite in the liver, spleen, and bone marrow of infected mice. There are currently only few studies on the potential of the Ace-DEX and its derivatives for the delivery of drugs against pathogens, and more studies are needed in the future to better understand how and to what extent acetalated dextran derivatives can be useful to formulate novel anti-infection formulations.

Conclusions and future perspectives

In conclusion, we have summarized the cutting-edge development of drug delivery systems based on Ac-DEX and its functional derivatives. The facile synthesis, along with the possibility for further chemical functionalization, makes Ac-DEX a versatile candidate for various therapeutic applications discussed in the previous sections. Compared with commercialized polymeric drug carriers, such as PLGA, Ac-DEX has a similar solubility profile, which makes it possible to fabricate by standardized procedures (single/double emulsion, nanoprecipitation, or electrospinning). Furthermore, the tunable pH-dependent release profile, biodegradability and biocompatibility are of particular interest for future clinical translations.

Despite the advantageous properties of Ac-DEX and derivatives, these polymers are still in the early stage of development, considering their relatively short research history. Like other polymeric material candidates, Ac-DEX and derivatives need to overcome many challenges before their clinical translations. First, the polymer synthesis and characterization need to be standardized, to minimize batch-to-batch variations. Considering the potential undesired hydrolysis of acetals on the polymer structure, the water exposure, especially acidic substance exposure, should be closely monitored in all steps, including polymer synthesis, particle fabrication and storage, to avoid unexpected polymer degradation. Second, we also need more reproducible and well-controlled particle production methods, to ensure the homogeneity of the particles with sufficient payload loading. To this end, the development and optimization of various techniques, such as microfluidic devices, electrospray and spray drying, is anticipated to support and speed-up the development and clinical translation of nanomedicines. In addition to particle fabrication, sterilization and long-term storage should be taken into consideration for clinical translations as well. Sterilization could be achieved by aseptic processing, or terminal sterilization techniques such as γ-irradiation. Regarding the storage, the promising preliminary results have shown Ac-DEX particles with bioactive enzyme payloads could be stored outside cold chain conditions for months as discussed in the previous sections. We would anticipate more storage stability test results of formulated biopharmaceuticals in specific applications. Last, but not least, the biosafety of the Ac-DEX-based delivery systems needs to be carefully evaluated, regarding the specific particle, the administration method and the desired application. Since there is no such "universal delivery platform" for different payloads, it is critical to focus on payload-specific delivery systems, and make critical assessments of bioavailability, biodistribution, and metabolic kinetics of the payloads using such Ac-DEX delivery systems. Considering the rapid development in the field, the innovative applications of Ac-DEX-based materials have great potential to be realized in the future.

Conflicts of interest

There are no conflicts to declare.

Acknowledgements

Notes and references

1 *IUPAC Compendium of Chemical Terminology*, ed. M. Nič, J. Jirát, B. Košata, A. Jenkins and A. McNaught, IUPAC, Research Triagle Park, NC, 2009.
2 T. Heinze, T. Liebert, B. Heublein and S. Hornig, *Polysaccharides II*, Springer Berlin Heidelberg, 2006, pp. 199–291.
3 R. Mehvar, *J. Controlled Release*, 2000, **69**, 1–25.
4 A. S. Volokhova, K. J. Edgar and J. B. Matson, *Mater. Chem. Front.*, 2020, **4**, 99–112.
5 F. Chen, G. Huang and H. Huang, *Int. J. Biol. Macromol.*, 2020, **145**, 827–834.
6 T. Miao, J. Wang, Y. Zeng, G. Liu and X. Chen, *Adv. Sci.*, 2018, **5**, 1700513.
7 M. A. Hussain, K. Abbas, I. Jantan and S. N. A. Bukhari, *Int. Mater. Rev.*, 2017, **62**, 78–98.
8 E. M. Bachelder, T. T. Beaudette, K. E. Broaders, J. Dashe and J. M. J. Fréchet, *J. Am. Chem. Soc.*, 2008, **130**, 10494–10495.
9 R. Gannimani, P. Walvekar, V. R. Naidu, T. M. Aminabhavi and T. Govender, *J. Controlled Release*, 2020, **328**, 736–761.
10 E. M. Bachelder, E. N. Pino and K. M. Ainslie, *Chem. Rev.*, 2017, **117**, 1915–1926.
11 K. E. Broaders, J. A. Cohen, T. T. Beaudette, E. M. Bachelder and J. M. J. Frechet, *Proc. Natl. Acad. Sci. U. S. A.*, 2009, **106**, 5497–5502.
12 K. J. Kauffman, C. Do, S. Sharma, M. D. Gallovic, E. M. Bachelder and K. M. Ainslie, *ACS Appl. Mater. Interfaces*, 2012, **4**, 4149–4155.
13 K. V. Hoang, H. M. Borteh, M. V. S. Rajaram, K. J. Peine, H. Curry, M. A. Collier, M. L. Homsy, E. M. Bachelder, J. S. Gunn, L. S. Schlesinger and K. M. Ainslie, *Int. J. Pharm.*, 2014, **477**, 334–343.
14 N. Chen, C. J. Kroger, R. M. Tisch, E. M. Bachelder and K. M. Ainslie, *Adv. Healthcare Mater.*, 2018, **7**, 1800341.
15 E. Graham-Gurysh, K. M. Moore, A. B. Satterlee, K. T. Sheets, F.-C. Lin, E. M. Bachelder, C. R. Miller, S. D. Hingtgen and K. M. Ainslie, *Mol. Pharmaceutics*, 2018, **15**, 1309–1318.
16 K. M. Moore, C. J. Batty, R. T. Stiepel, C. J. Genito, E. M. Bachelder and K. M. Ainslie, *ACS Appl. Mater. Interfaces*, 2020, **12**, 38950–38961.
17 R. Watkins-Schulz, P. Tiet, M. D. Gallovic, R. D. Junkins, C. Batty, E. M. Bachelder, K. M. Ainslie and J. P. Y. Ting, *Biomaterials*, 2019, **205**, 94–105.
18 E. T. Graham and K. E. Broaders, *Biomacromolecules*, 2019, **20**, 2008–2014.
19 J. L. Cohen, S. Schubert, P. R. Wich, L. Cui, J. A. Cohen, J. L. Mynar and J. M. J. Frechet, *Bioconjugate Chem.*, 2011, **22**, 1056–1065.
20 H. X. Nguyen and E. A. O'Reara, *J. Microencapsulation*, 2017, **34**, 299–307.

21 D. Bamberger, D. Hobernik, M. Konhaeuser, M. Bros and P. R. Wich, *Mol. Pharmaceutics*, 2017, **14**, 4403–4416.

22 M. P. A. Ferreira, S. Ranjan, S. Kinnunen, A. Correia, V. Talman, E. Mäkilä, B. Barrios-Lopez, M. Kemell, V. Balasubramanian, J. Salonen, J. Hirvonen, H. Ruskoaho, A. J. Airaksinen and H. A. Santos, *Small*, 2017, **13**, 1701276.

23 G. Torrieri, F. Fontana, P. Figueiredo, Z. Liu, M. P. A. Ferreira, V. Talman, J. P. Martins, M. Fusciello, K. Moslova, T. Teesalu, V. Cerullo, J. Hirvonen, H. Ruskoaho, V. Balasubramanian and H. A. Santos, *Nanoscale*, 2020, **12**, 2350–2358.

24 K. Butzbach, M. Konhäuser, M. Fach, D. Bamberger, B. Breitenbach, B. Epe and P. Wich, *Polymers*, 2019, **11**, 896.

25 M. Tizzotti, A. Charlot, E. Fleury, M. Stenzel and J. Bernard, *Macromol. Rapid Commun.*, 2010, **31**, 1751–1772.

26 H. T. T. Duong, F. Hughes, S. Sagnella, M. Kavallaris, A. Macmillan, R. Whan, J. Hook, T. P. Davis and C. Boyer, *Mol. Pharmaceutics*, 2012, **9**, 3046–3061.

27 G. Moad, E. Rizzardo and S. H. Thang, *Polymer*, 2008, **49**, 1079–1131.

28 S. Wannasarit, S. Wang, P. Figueiredo, C. Trujillo, F. Eburnea, L. Simón-Gracia, A. Correia, Y. Ding, T. Teesalu, D. Liu, R. Wiwattanapatapee, H. A. Santos and W. Li, *Adv. Funct. Mater.*, 2019, **29**, 1905352.

29 S. Wang, S. Wannasarit, P. Figueiredo, J. Li, A. Correia, B. Xia, R. Wiwattanapatapee, J. Hirvonen, D. Liu, W. Li and H. A. Santos, *Mater. Horiz.*, 2020, **7**, 1573–1580.

30 J. E. Hein and V. V. Fokin, *Chem. Soc. Rev.*, 2010, **39**, 1302–1315.

31 B. B. Breitenbach, I. Schmid and P. R. Wich, *Biomacromolecules*, 2017, **18**, 2839–2848.

32 H. Kuang, Y. Wu, Z. Zhang, J. Li, X. Chen, Z. Xie, X. Jing and Y. Huang, *Polym. Chem.*, 2015, **6**, 3625–3633.

33 Z. Zhang, X. Chen, L. Chen, S. Yu, Y. Cao, C. He and X. Chen, *ACS Appl. Mater. Interfaces*, 2013, **5**, 10760–10766.

34 B. B. Breitenbach, E. Steiert, M. Konhäuser, L.-M. Vogt, Y. Wang, S. H. Parekh and P. R. Wich, *Soft Matter*, 2019, **15**, 1423–1434.

35 B. Shkodra-Pula, C. Kretzer, P. M. Jordan, P. Klemm, A. Koeberle, D. Pretzel, E. Banoglu, S. Lorkowski, M. Wallert, S. Höppener, S. Stumpf, A. Vollrath, S. Schubert, O. Werz and U. S. Schubert, *J. Nanobiotechnol.*, 2020, **18**, 73.

36 F. Kong, H. Zhang, X. Zhang, D. Liu, D. Chen, W. Zhang, L. Zhang, H. A. Santos and M. Hai, *Adv. Funct. Mater.*, 2016, **26**, 6158–6169.

37 D. Liu, H. Zhang, E. Mäkilä, J. Fan, B. Herranz-Blanco, C.-F. Wang, R. Rosa, A. J. Ribeiro, J. Salonen, J. Hirvonen and H. A. Santos, *Biomaterials*, 2015, **39**, 249–259.

38 Z. Liu, Y. Li, W. Li, C. Xiao, D. Liu, C. Dong, M. Zhang, E. Mäkilä, M. Kemell, J. Salonen, J. T. Hirvonen, H. Zhang, D. Zhou, X. Deng and H. A. Santos, *Adv. Mater.*, 2018, **30**, 1703393.

39 S. Wang, S. Wannasarit, P. Figueiredo, G. Molinaro, Y. Ding, A. Correia, L. Casettari, R. Wiwattanapatapee, J. Hirvonen, D. Liu, W. Li and H. A. Santos, *Adv. Ther.*, 2020, **2000058**.

40 D. Liu, C. R. Bernuz, J. Fan, W. Li, A. Correia, J. Hirvonen and H. A. Santos, *Adv. Funct. Mater.*, 2017, **27**, 1604508.

41 M. P. A. Ferreira, V. Talman, G. Torrieri, D. Liu, G. Marques, K. Moslova, Z. Liu, J. F. Pinto, J. Hirvonen, H. Ruskoaho and H. A. Santos, *Adv. Funct. Mater.*, 2018, **28**, 1705134.

42 M. M. Johnson, M. A. Collier, K. V. Hoang, E. N. Pino, E. G. Graham-Gurysh, M. D. Gallovic, M. S. H. Zahid, N. Chen, L. Schlesinger, J. S. Gunn, E. M. Bachelder and K. M. Ainslie, *Mol. Pharmaceutics*, 2018, **15**, 5336–5348.

43 R. Vasiliauskas, D. Liu, S. Cito, H. Zhang, M.-A. Shahbazi, T. Sikanen, L. Mazutis and H. A. Santos, *ACS Appl. Mater. Interfaces*, 2015, **7**, 14822–14832.

44 T. Bauleth-Ramos, M.-A. Shahbazi, D. Liu, F. Fontana, A. Correia, P. Figueiredo, H. Zhang, J. P. Martins, J. T. Hirvonen, P. Granja, B. Sarmento and H. A. Santos, *Adv. Funct. Mater.*, 2017, **27**, 1703303.

45 K. J. Peine, M. Guerau-de-Arellano, P. Lee, N. Kanthamneni, M. Severin, G. D. Probst, H. Peng, Y. Yang, Z. Vangundy, T. L. Papenfuss, A. E. Lovett-Racke, E. M. Bachelder and K. M. Ainslie, *Mol. Pharmaceutics*, 2014, **11**, 828–835.

46 E. A. T. Guzman, Q. Sun and S. A. Meenach, *ACS Biomater. Sci. Eng.*, 2019, **5**, 6570–6580.

47 Z. Wang and S. A. Meenach, *J. Pharm. Sci.*, 2017, **106**, 3539–3547.

48 A. D. Duong, S. Sharma, K. J. Peine, G. Gupta, A. R. Satoskar, E. M. Bachelder, B. E. Wyslouzil and K. M. Ainslie, *Mol. Pharmaceutics*, 2013, **10**, 1045–1055.

49 M. A. A. Collier, R. D. D. Junkins, M. D. D. Gallovic, B. M. M. Johnson, M. M. M. Johnson, A. N. N. MacIntyre, G. D. D. Sempowski, E. M. M. Bachelder, J. P. Y. P.-Y. Ting and K. M. M. Ainslie, *Mol. Pharmaceutics*, 2018, **15**, 4933–4946.

50 J. V. Gregory, D. R. Vogus, A. Barajas, M. A. Cadena, S. Mitragotri and J. Lahann, *Adv. Healthcare Mater.*, 2020, **9**, 2000564.

51 C. J. Martínez Rivas, M. Tarhini, W. Badri, K. Miladi, H. Greige-Gerges, Q. A. Nazari, S. A. Galindo Rodríguez, R. Á. Román, H. Fessi and A. Elaissari, *Int. J. Pharm.*, 2017, **532**, 66–81.

52 Z. Liu, F. Fontana, A. Python, J. T. Hirvonen and H. A. Santos, *Small*, 2020, **16**, 1904673.

53 D. Liu, H. Zhang, F. Fontana, J. T. Hirvonen and H. A. Santos, *Lab Chip*, 2017, **17**, 1856–1883.

54 D. Liu, S. Cito, Y. Zhang, C.-F. Wang, T. M. Sikanen and H. A. Santos, *Adv. Mater.*, 2015, **27**, 2298–2304.

55 D. Liu, H. Zhang, F. Fontana, J. T. Hirvonen and H. A. Santos, *Adv. Drug Delivery Rev.*, 2018, **128**, 54–83.

56 S. Bertoni, Z. Liu, A. Correia, J. P. Martins, A. Rahikkala, F. Fontana, M. Kemell, D. Liu, B. Albertini, N. Passerini, W. Li and H. A. Santos, *Adv. Funct. Mater.*, 2018, **28**, 1806175.

57 R. Karnik, F. Gu, P. Basto, C. Cannizzaro, L. Dean, W. Kyei-Manu, R. Langer and O. C. Farokhzad, *Nano Lett.*, 2008, **8**, 2906–2912.

58 Y. Song, J. Hormes and C. S. S. R. Kumar, *Small*, 2008, **4**, 698–711.

59 H. Song and R. F. Ismagilov, *J. Am. Chem. Soc.*, 2003, **125**, 14613–14619.

60 D. Liu, H. Zhang, S. Cito, J. Fan, E. Mäkilä, J. Salonen, J. Hirvonen, T. M. Sikanen, D. A. Weitz and H. A. Santos, *Nano Lett.*, 2017, **17**, 606–614.

61 F. Fontana, M.-A. Shahbazi, D. Liu, H. Zhang, E. Mäkilä, J. Salonen, J. T. Hirvonen and H. A. Santos, *Adv. Mater.*, 2017, **29**, 1603239.

62 D. J. McClements, *Curr. Opin. Colloid Interface Sci.*, 2012, **17**, 235–245.

63 T. Tadros, P. Izquierdo, J. Esquena and C. Solans, *Adv. Colloid Interface Sci.*, 2004, **108–109**, 303–318.

64 K. J. J. Kauffman, N. Kanthamneni, S. A. A. Meenach, B. C. C. Pierson, E. M. M. Bachelder and K. M. M. Ainslie, *Int. J. Pharm.*, 2012, **422**, 356–363.

65 D. Liu, J. Chen, T. Jiang, W. Li, Y. Huang, X. Lu, Z. Liu, W. Zhang, Z. Zhou, Q. Ding, H. A. Santos, G. Yin and J. Fan, *Adv. Mater.*, 2018, **30**, 1706032.

66 J. P. Martins, G. Torrieri and H. A. Santos, *Expert Opin. Drug Deliv.*, 2018, **15**, 469–479.

67 S. Poozesh and E. Bilgili, *Int. J. Pharm.*, 2019, **562**, 271–292.

68 A. Singh and G. Van den Mooter, *Adv. Drug Delivery Rev.*, 2016, **100**, 27–50.

69 S. A. Meenach, Y. J. Kim, K. J. Kauffman, N. Kanthamneni, E. M. Bachelder and K. M. Ainslie, *Mol. Pharmaceutics*, 2012, **9**, 290–298.

70 Z. Wang and S. A. Meenach, *Pharm. Res.*, 2016, **33**, 1862–1872.

71 N. K. Shah, Z. Wang, S. K. Gupta, A. Le Campion and S. A. Meenach, *Pharm. Dev. Technol.*, 2019, **24**, 1133–1143.

72 Z. Wang, S. K. Gupta and S. A. Meenach, *Int. J. Pharm.*, 2017, **525**, 264–274.

73 Z. Wang, J. L. Cuddigan, S. K. Gupta and S. A. Meenach, *Int. J. Pharm.*, 2016, **512**, 305–313.

74 R. T. Steipel, M. D. Gallovic, C. J. Batty, E. M. Bachelder and K. M. Ainslie, *Mater. Sci. Eng., C*, 2019, **105**, 110070.

75 N. Nikolaou and T. Krasia-Christoforou, *Eur. J. Pharm. Sci.*, 2018, **113**, 29–40.

76 N. Chen, M. M. Johnson, M. A. Collier, M. D. Gallovic, E. M. Bachelder and K. M. Ainslie, *J. Controlled Release*, 2018, **273**, 147–159.

77 M. D. Gallovic, K. L. Schully, M. G. Bell, M. A. Elberson, J. R. Palmer, C. A. Darko, E. M. Bachelder, B. E. Wyslouzil, A. M. Keane-Myers and K. M. Ainslie, *Adv. Healthcare Mater.*, 2016, **5**, 2617–2627.

78 R. D. Junkins, M. D. Gallovic, B. M. Johnson, M. A. Collier, R. Watkins-Schulz, N. Cheng, C. N. David, C. E. McGee, G. D. Sempowski, I. Shterev, K. McKinnon, E. M. Bachelder, K. M. Ainslie and J. P.-Y. Ting, *J. Controlled Release*, 2018, **270**, 1–13.

79 N. Chen, M. A. Collier, M. D. Gallovic, G. C. Collins, C. C. Sanchez, E. Q. Fernandes, E. M. Bachelder and K. M. Ainslie, *Int. J. Pharm.*, 2016, **512**, 147–157.

80 Y. Fu, W. Liu, L. Wang, B. Zhu, M. Qu, L. Yang, X. Sun, T. Gong, Z. Zhang, Q. Lin and L. Zhang, *Adv. Funct. Mater.*, 2018, **28**, 1802250.

81 L. R. Volpatti, M. A. Matranga, A. B. Cortinas, D. Delcassian, K. B. Daniel, R. Langer and D. G. Anderson, *ACS Nano*, 2020, **14**, 488–497.

82 T.-H. Park, T. W. Eyster, J. M. Lumley, S. Hwang, K. J. Lee, A. Misra, S. Rahmani and J. Lahann, *Small*, 2013, **9**, 3051–3057.

83 M. L. Viger, W. Sheng, K. Dore, A. H. Alhasan, C.-J. Carling, J. Lux, C. de, G. Lux, M. Grossman, R. Malinow and A. Almutairi, *ACS Nano*, 2014, **8**, 4815–4826.

84 F. Fontana, P. Figueiredo, T. Bauleth-Ramos, A. Correia and H. A. Santos, *Small Methods*, 2018, **2**, 1700347.

85 E. M. Bachelder, T. T. Beaudette, K. E. Broaders, J. M. J. Frechet, M. T. Albrecht, A. J. Mateczun, K. M. Ainslie, J. T. Pesce and A. M. Keane-Myers, *Mol. Pharmaceutics*, 2010, **7**, 826–835.

86 K. J. Peine, E. M. Bachelder, Z. Vangundy, T. Papenfuss, D. J. Brackman, M. D. Gallovic, K. Schully, J. Pesce, A. Keane-Myers and K. M. Ainslie, *Mol. Pharmaceutics*, 2013, **10**, 2849–2857.

87 N. Kanthamneni, S. Sharma, S. A. Meenach, B. Billet, J.-C. Zhao, E. M. Bachelder and K. M. Ainslie, *Int. J. Pharm.*, 2012, **431**, 101–110.

88 K. L. Schully, S. Sharma, K. J. Peine, J. Pesce, M. A. Elberson, M. E. Fonseca, A. M. Prouty, M. G. Bell, H. Borteh, M. Gallovic, E. M. Bachelder, A. Keane-Myers and K. M. Ainslie, *Pharm. Res.*, 2013, **30**, 1349–1361.

89 N. Chen, M. D. Gallovic, P. Tiet, J. P.-Y. P. Y. Ting, K. M. Ainslie and E. M. Bachelder, *J. Controlled Release*, 2018, **289**, 114–124.

90 R. T. Stiepel, C. J. Batty, C. A. MacRaild, R. S. Norton, E. Bachelder and K. M. Ainslie, *Int. J. Pharm.*, 2021, **593**, 120168.

91 A. Davidson and B. Diamond, *N. Engl. J. Med.*, 2001, **345**, 340–350.

92 F. L. Vigario, J. Kuiper and B. Slütter, *EBioMedicine*, 2020, **57**, 102827.

93 C. L. Stabler, Y. Li, J. M. Stewart and B. G. Keselowsky, *Nat. Rev. Mater.*, 2019, **4**, 429–450.

94 N. Chen, K. J. Peine, M. A. Collier, S. Gautam, K. A. Jablonski, M. Guerau-de-Arellano, K. M. Ainslie and E. M. Bachelder, *Adv. Biosyst.*, 2017, **1**, 1700022.

95 M. Fusciello, F. Fontana, S. Tähtinen, C. Capasso, S. Feola, B. Martins, J. Chiaro, K. Peltonen, L. Ylösmäki, E. Ylösmäki, F. Hamdan, O. K. Kari, J. Ndika, H. Alenius, A. Urtti, J. T. Hirvonen, H. A. Santos and V. Cerullo, *Nat. Commun.*, 2019, **10**, 1–13.

96 F. Fontana, M. Fusciello, C. Groeneveldt, C. Capasso, J. Chiaro, S. Feola, Z. Liu, E. M. Mäkilä, J. J. Salonen, J. T. Hirvonen, V. Cerullo and H. A. Santos, *ACS Nano*, 2019, **13**, 6477–6490.

97 Y. Shi, R. van der Meel, X. Chen and T. Lammers, *Theranostics*, 2020, **10**, 7921–7924.

98 D. Sun, S. Zhou and W. Gao, *ACS Nano*, 2020, **14**, 12281–12290.

99 A. Nel, E. Ruoslahti and H. Meng, *ACS Nano*, 2017, **11**, 9567–9569.

100 S. Wilhelm, A. J. Tavares, Q. Dai, S. Ohta, J. Audet, H. F. Dvorak and W. C. W. Chan, *Nat. Rev. Mater.*, 2016, **1**, 16014.

101 B. Dai, X. Wu, C. J. Butch, J. Wang, Z. Wang, Y. Wang, S. Nie, Q. Lu, Y. Wang and Y. Ding, *Nano Res.*, 2019, **12**, 1959–1966.

102 C. B. Braga, L. A. Kido, E. N. Lima, C. A. Lamas, V. H. A. Cagnon, C. Ornelas and R. A. Pilli, *ACS Biomater. Sci. Eng.*, 2020, **6**, 2929–2942.

103 W. C. Widdison, S. D. Wilhelm, E. E. Cavanagh, K. R. Whiteman, B. A. Leece, Y. Kovtun, V. S. Goldmacher, H. Xie, R. M. Steeves, R. J. Lutz, R. Zhao, L. Wang, W. A. Blättler and R. V. J. Chari, *J. Med. Chem.*, 2006, **49**, 4392–4408.

104 H. Zhang, D. Liu, L. Wang, Z. Liu, R. Wu, A. Janoniene, M. Ma, G. Pan, L. Baranauskiene, L. Zhang, W. Cui, V. Petrikaite, D. Matulis, H. Zhao, J. Pan and H. A. Santos, *Adv. Healthcare Mater.*, 2017, **6**, 1601406.

105 J. Nam, S. Son, K. S. Park, W. Zou, L. D. Shea and J. J. Moon, *Nat. Rev. Mater.*, 2019, **4**, 398–414.

106 B. J. Moeller, R. A. Richardson and M. W. Dewhirst, *Cancer Metastasis Rev.*, 2007, **26**, 241–248.

107 Y. Wang, Y. Xie, J. Li, Z.-H. Peng, Y. Sheinin, J. Zhou and D. Oupický, *ACS Nano*, 2017, **11**, 2227–2238.

108 X. Li, N. Kwon, T. Guo, Z. Liu and J. Yoon, *Angew. Chem., Int. Ed.*, 2018, **57**, 11522–11531.

109 R. Song, S. Peng, Q. Lin, M. Luo, H. Y. Chung, Y. Zhang and S. Yao, *Langmuir*, 2019, **35**, 10166–10172.

110 M. Gao, C. Liang, X. Song, Q. Chen, Q. Jin, C. Wang and Z. Liu, *Adv. Mater.*, 2017, **29**, 1701429.

111 M. Garcia, S. L. Mulvagh, C. N. B. Merz, J. E. Buring and J. A. E. Manson, *Circ. Res.*, 2016, **118**, 1273–1293.

112 M. H. Criqui and V. Aboyans, *Circ. Res.*, 2015, **116**, 1509–1526.

113 P. Bhatnagar, K. Wickramasinghe, E. Wilkins and N. Townsend, *Heart*, 2016, **102**, 1945–1952.

114 S. Suarez, G. N. Grover, R. L. Braden, K. L. Christman and A. Amutairi, *Biomacromolecules*, 2013, **14**, 3927–3935.

115 S. L. Suarez, A. Munoz, A. C. Mitchell, R. L. Braden, C. Luo, J. R. Cochran, A. Almutairi and K. L. Christman, *ACS Biomater. Sci. Eng.*, 2016, **2**, 197–204.

116 M. Shin, H.-A. Lee, M. Lee, Y. Shin, J.-J. Song, S.-W. Kang, D.-H. Nam, E. J. Jeon, M. Cho, M. Do, S. Park, M. S. Lee, J.-H. Jang, S.-W. Cho, K.-S. Kim and H. Lee, *Nat. Biomed. Eng.*, 2018, **2**, 304–317.

117 H.-N. Kim and J. L. Januzzi, *Circulation*, 2011, **123**, 2015–2019.

118 A. S. Maisel, P. Krishnaswamy, R. M. Nowak, J. McCord, J. E. Hollander, P. Duc, T. Omland, A. B. Storrow, W. T. Abraham, A. H. B. Wu, P. Clopton, P. G. Steg, A. Westheim, C. W. Knudsen, A. Perez, R. Kazanegra, H. C. Herrmann and P. A. McCullough, *N. Engl. J. Med.*, 2002, **347**, 161–167.

119 L. R. Potter, A. R. Yoder, D. R. Flora, L. K. Antos and D. M. Dickey, *Handbook of Experimental Pharmacology*, 2009, pp. 341–366.

120 H. Uosaki, A. Magadum, K. Seo, H. Fukushima, A. Takeuchi, Y. Nakagawa, K. W. Moyes, G. Narazaki, K. Kuwahara, M. Laflamme, S. Matsuoka, N. Nakatsuji, K. Nakao, C. Kwon, D. A. Kass, F. B. Engel and J. K. Yamashita, *Circ.: Cardiovasc. Genet.*, 2013, **6**, 624–633.

121 L. Paasonen, S. Sharma, G. B. Braun, V. R. Kotamraju, T. D. Y. Chung, Z.-G. She, K. N. Sugahara, M. Yliperttula, B. Wu, M. Pellecchia, E. Ruoslahti and T. Teesalu, *ChemBioChem*, 2016, **17**, 570–575.

122 L. Wang, C. Hu and L. Shao, *Int. J. Nanomedicine*, 2017, **12**, 1227–1249.

123 M. J. Hajipour, K. M. Fromm, A. Akbar Ashkarran, D. Jimenez de Aberasturi, I. R. de Larramendi, T. Rojo, V. Serpooshan, W. J. Parak and M. Mahmoudi, *Trends Biotechnol.*, 2012, **30**, 499–511.

124 K. V. Hoang, H. Curry, M. A. Collier, H. Borteh, E. M. Bachelder, L. S. Schlesinger, J. S. Gunn and K. M. Ainslie, *Antimicrob. Agents Chemother.*, 2016, **60**, 2052–2062.

125 M. A. Collier, K. J. Peine, S. Gautam, S. Oghumu, S. Varikuti, H. Borteh, T. L. Papenfuss, A. R. Sataoskar, E. M. Bachelder and K. M. Ainslie, *Int. J. Pharm.*, 2016, **499**, 186–194.